State Space Modeling for 3-D Variation Propagation in Rigid-Body Multistage Assembly Processes

Jian Liu, Jionghua Jin, *Member, IEEE*, and Jianjun Shi

***Abstract*—Dimensional variation propagation modeling is a critical enabling technique for product quality variation reduction in a multistage assembly process (MAP). However, the complex inter-stage correlations make the modeling extremely difficult. This paper aims to improve the existing techniques by developing a generic state space approach to modeling 3-D variation propagation induced by various types of variation sources in general MAPs. A concept of differential motion vector (DMV) is adopted to represent deviations with respect to four types of coordinate systems and to formulate the variation propagation as a series of homogeneous transformation among different coordinate systems. Based on this representation and formulation strategy, a novel generic mechanism is proposed to model the effect of variations induced by part fabrication processes and a MAP. A case study on 3-D variation propagation in a panel fitting process is presented to demonstrate the modeling and analysis capability of the proposed methodology.**

***Note to Practitioners*—This paper was motivated by the timely need for effective variation reduction in a MAP. In such a process, variations from fixtures, assembly operations, and individual parts may be induced and propagated along assembly stages to affect product dimensional quality. It is critical and challenging to model complex variation propagation for identifying the variation sources and improving product quality. Although commercial products offer 3-D variation analysis functionality, there is no explicit model that links product/process design and product quality. Some research has been done to model 3-D variation propagation in multistage machining or assembly processes for 3-2-1 fixturing schemes. However, variations induced by the features on pre-fabricated parts are not explicitly considered. This paper developed a generic modeling approach by using DMV representation. Complex 3-D variation propagation is mathematically modeled by a series of linear transformations of DMVs among four types of coordinate systems, which are defined as general frameworks for reference, fixtures, parts, and features on parts. The model is represented in a state space model format, in which all system matrices are explicitly defined through utilizing the available product design and assembly process plan information. Physical experiments are presented to validate the model in production.**

Manuscript received November 15, 2008. First published May 15, 2009; current version published April 07, 2010. This paper was recommended for publication by Associate Editor J. Li and Editor M. Wang upon evaluation of the reviewers' comments. This work was supported in part by the Engineering Research Center for Reconfigurable Manufacturing Systems under National Science Foundation (NSF) Grant EEC-9529125 at the University of Michigan, and in part by the NSF under Grant PECASE/CAREER AWARD DMII-0133942.

J. Liu is with the Department of Systems and Industrial Engineering, University of Arizona, Tucson, AZ 85718 USA (e-mail: jianliu@sie.arizona.edu).

J. Jin is with the Department of Industrial and Operations Engineering, University of Michigan, Ann Arbor, MI 48109 USA (e-mail: jhjin@umich.edu).

J. Shi is with the H. Milton Stewart School of Industrial and Systems Engineering, Georgia Institute of Technology, Atlanta, GA 30332 USA (e-mail: jianjun.shi@isye.gatech.edu).

Color versions of one or more of the figures in this paper are available online at http://ieeexplore.ieee.org.

Digital Object Identifier 10.1109/TASE.2009.2012435

***Index Terms*—Differential motion vector, dimensional variation propagation, multistage assembly process, state space model.**

NOMENCLATURE

N	Number of stages in a MAP.
S	Number of parts to be assembled.
J_k	Number of fixtures used at stage k.
R	Reference coordinate system.
${}^0F_{k,j}, F_{k,j}$	Nominal, actual fixture coordinate system of fixture j at stage k.
P_r	Part coordinate system of part r.
$\mathbf{x}_{CS_1}^{CS_2}$	Differential motion vector of CS_1 w.r.t. CS_2.
$\mathrm{p1}, \mathrm{p2}, \mathrm{p3}$	Three datum features that compose the primary datum surface of a fixturing scheme.
$\mathrm{s1}, \mathrm{s2}$	Two datum features that compose the secondary datum surface of a fixturing scheme.
t	Tertiary datum surface of a fixturing scheme.
$\bullet,\ k,\ j$	Datum feature $\bullet, \bullet \in \{\mathrm{p1}, \mathrm{p2}, \mathrm{p3}, \mathrm{s1}, \mathrm{s2}, \mathrm{t}\}$, of fixture j at stage k.
$T_{\bullet,k,j}$	Local Coordinate System of datum feature "$\bullet,\ k,\ j$."
$\mathrm{L}_1, \mathrm{L}_2, \mathrm{L}_3$	Three fixture locators touching the primary datum surface of the part/subassembly.
$\mathrm{P}_1, \mathrm{P}_2$	Two fixture locators touching the secondary datum surface of the part/subassembly.
P_3	Fixture locator touching the tertiary datum surface of the part/subassembly.
$\circ,\ k,\ j$	Fixture locator $\circ, \circ \in \{\mathrm{L}_1, \mathrm{L}_2, \mathrm{L}_3, \mathrm{P}_1, \mathrm{P}_2, \mathrm{P}_3\}$, of fixture j at stage k.
$T_{\circ,k,j}$	Local coordinate system of a feature that serves as "$\circ,\ k,\ j$."
$*, k, m$	Feature $*, * = 1, 2, \ldots, M_{k,m}$, that serves as the $*$th feature involved in calculating the mth Key Product Characteristic (KPC) measured at stage k.
$T_{*,\ k,\ m}$	Local Coordinate System of datum feature "$*,\ k,\ m$."
$i(\bullet, k, j)$	Function indicating the index of the part that contains datum feature "$\bullet, k, j$."
$P_{i(\bullet,k,j)}$	Part coordinate system of the part that contains datum feature "$\bullet,\ k,\ j$."

$r(c,k,j)$	Function indicating the index of the part who is the cth part on the subassembly located by fixture j at stage k.
$P_{r(c,k,j)}$	Part coordinate system of the part $r(c,k,j)$.
M_k	Number of KPCs measured at stage k.
$M_{k,m}$	Number of features involved in calculating the mth KPC at stage k.
$l_{k,j}$	Number of parts on a subassembly that are located by fixture j at stage k.

I. Introduction

MULTISTAGE assembly processes (MAPs) are widely adopted in manufacturing industry to deliver products with complex designated functionalities. In a MAP, parts or subassemblies are assembled together through a series of operations executed at multiple stages to form a final assembled product. The quality of the final products is reflected by a set of measurements of Key Product Characteristics (KPCs) which are defined as dimensions referenced by the design datums or features on different parts of an assembly. High quality KPCs can be achieved when all parts are located in the correct design positions and orientations with respect to (w.r.t.) the six spatial degrees of freedom. However, due to imperfections in assembly stages, e.g., fixture locators' deviations from the nominal positions and/or part features' deviations from the nominal geometry, assembly errors may be introduced and cause random deviations of KPC measurements from their designated nominal values. As some features generated in upstream stages of a MAP are used as the datum features in downstream stages, these deviations will be propagated and accumulated, leading to large variations on the KPCs of final assembled products, or even severe interferences among parts and/or subassemblies.

Reducing the dimensional variations is an essential issue for improving product quality as well as the productivity of a MAP. It is greatly beneficial to develop a systematic variation reduction strategy by monitoring process consistency and identifying the variation sources based on available online KPC measurements. In order to implement this strategy, it is desirable to build a generic mathematical model that directly links variation of KPCs and that of the process variation sources.

With the rapid advancement of sensing and computer technology, online automatic measurement devices are widely implemented to perform 100% inspection with tremendous data streams [1]. However, complex interactions between KPC measurements and potential process variation sources and the inter-correlation among different assembly stages make it extremely challenging to effectively utilize those data streams for the variation reduction purpose. Therefore, the development of a mathematical model, which can fully represent the quality-process interactions and variation propagation, is considered as the first critical step of variation reduction.

The recent decade has witnessed the development of variation propagation modeling methodologies, which can be divided into two categories: statistical modeling and engineering modeling. Statistical modeling methods construct variation propagation models from historical quality measurement data collected at all stages in a MAP. Lawless *et al.* [2] and Agrawal *et al.* [3] investigated the variation transmission issues in multistage manufacturing processes by constructing AR(1) models in a state space format. The estimated model coefficients are used to describe the inter-correlation among the KPCs from two adjacent stages. Based on KPC measurements, these statistical models assist engineers in understanding inter-stage correlations among part quality measurements. However, they limited their diagnostic capability since the effects of the process variation sources on KPC variations are not represented.

Different from statistical modeling techniques, engineering variation propagation modeling is conducted based on engineering domain knowledge, rather than measurement data. The essence of engineering modeling is to mathematically represent quality-process interactions and inter-stage correlation in a series of equations based on product/process design, e.g., computer-aided design (CAD) and computer-aided manufacturing (CAM). For assembly processes, Mantripragada and Whitney [4] proposed a concept of datum flow chain (DFC) to capture the underlying datum logic, at an abstract level. Assembly processes can be classified into two types: 1) Type-I, which assembles parts together according completely to their prefabricated mating features, e.g., furniture assembly; and 2) Type-II, which achieves final assembly by welding or riveting parts located by fixtures according to a predefined DFC, e.g., automotive and aircraft body assembly. The method for modeling the variation propagation in these two types of assembly process was introduced by Mantripragada and Whitney [5] from a perspective of assembly structure design. However, the explicit model derivation procedure was not discussed. Jin and Shi [6] proposed state space modeling techniques for 2-D sheet metal assembly, without taking into account the 3-D Type-I assembly operation. A state space model was adopted by Huang *et al.* [7] to model 3-D variation propagation in multistage machining processes, with an approximate linearization strategy. Zhou *et al.* further improved the modeling technique by providing explicit expressions for deriving all system matrices in the model. Differential motion vectors (DMV), a concept widely used in robotics, was adopted as the state vectors to represent the location and orientation deviations of KPCs [8]. Recently, Huang *et al.* [9] developed a generic 3-D variation model for a group of locating schemes.

Although 3-D variation propagation model has been significantly improved, a more generic approach is still needed to overcome their limitations. For instance, the method in [8] and [9] can model a datum surface with a single feature. This is reasonable for machining processes. However, in an assembly process, a datum surface is often composed of multiple features on different parts. Modeling of this situation is not explicitly considered by [8] and [9]. Also, the definition of state vector is of great importance to form a generic state space model. DMV components of the state vectors used in [8] are for individual features. If this definition strategy is adopted in modeling a MAP, the number of parts and features is generally very large and thus significantly increase the dimension of the state vector. Thus, a new state vector needs to be defined to control the dimension of the state vector. In [9], the state vectors are defined as a stack-up of vectorial deviations of parts' reference points. For different stages, the definitions of state vectors are different. This strategy

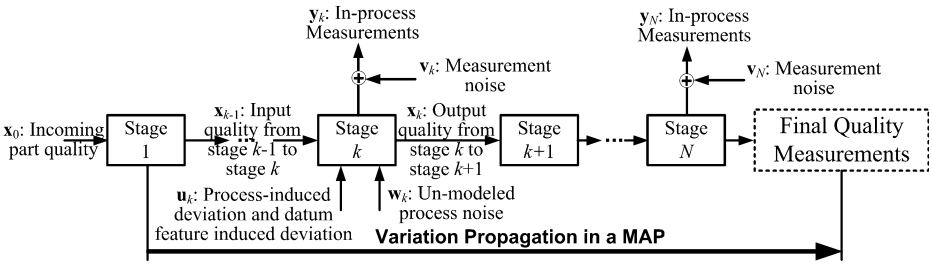

Fig. 1. Illustration of deviation transmission in a MAP.

makes it difficult to develop a generic procedure for deriving system matrices at different stages. Finally, variations of features on parts, including the features used as datum features, mating features or the measurement features, are inevitable in their fabrication processes. However, the impacts of this type of variation sources are not explicitly modeled in [8] and [9].

In this paper, a generic state space modeling method is developed to mathematically describe 3-D variation propagation in a general rigid-body MAP. Differential Motion Vectors (DMVs) are adopted to represent the random deviations of parts as state vectors, and that of variation sources as input vectors. The physics of variation induction and transmission are described by a series of control matrices and dynamic matrices. These model coefficient matrices are derived as the functions of the product and process design parameters, according to a series of lemmas and corollaries. The lemmas and corollaries provide a generic basis for describing a wide variety of assembly processes and modeling more variation propagation scenarios, such as the variation induced by part fabrication processes, which cannot be modeled by the existing modeling techniques.

The state space model has great impacts on systematic variation reduction. First, the proposed model mathematically links the random deviations of the inputs, the variation sources, with the outputs, the quality of KPCs. Based on the given product/process variation information, the model can be used to explicitly derive the means and variances/covariance of KPCs. Although the same functionality can be implemented by the software packages [10]–[12] that are built upon commonly accepted GD&T standards[13] and computer-aided tolerancing methodologies [14], [15], the explicit process-level models are not provided to users. As a result, a time-consuming Monte Carlo (MC) simulation has to be conducted to estimate the KPC distribution parameters. Second, although some commercial tool provide a model to describe the process input/output relationship, they are often generated with "MC-based simulation tool" for a given process design [9]. Moreover, model coefficients are not explicitly linked with the product/process design parameters. The process-specific model can only be used to benchmark various process options and to identify the best one among the trials. The proposed state space model explicitly represents the model coefficients as functions of product/process design parameters, such as fixture configuration and process sequencing. This explicit representation can be further applied in optimal design of products and processes, such as system-level fixture layout design. Thus, it creates tremendous potentials for improving the quality of MAP design. Finally, the model can also be used to conduct process diagnosis and sensor placement optimization, where classical concepts from the control theory, such as the "observability," can be applied to solve the problem.

The remainder of this paper is organized as follows: Section II introduces the mathematical representations of various types of deviations in a MAP. The detail modeling procedure is presented in Section III. A case study of a real-world MAP is presented in Section IV to validate the proposed model in analyzing dimensional variation of product quality. Concluding remarks and potential applications of the proposed modeling technique are discussed in Section V.

II. Geometrical Representation

An assembly process is used to attach interchangeable parts together in a sequential manner to create a finished product with complicated structure that cannot be obtained by other fabrication processes. Depending on the complexity of the product, an assembly process consists of multiple stages, each of which assembles two or more parts and/or subassemblies that are located by either fixtures or matting features on other parts. If any deviation occurs on a fixture locator, or a matting feature, dimensional deviations will be generated on some features of the subassembly. These faulty features will transmit the deviations to downstream stages through DFC. At some stages, KPC measurements are taken to monitor product quality. This series of KPC measurements data carries all the information of process deviations and their transmission along multiple stages, as illustrated by Fig. 1. To study the nature of this complicated deviation transmission, it is necessary to mathematically represent all types of deviations.

A. Coordinate Systems Definition

There are three types of elements involved in the deviation transmission: fixtures, parts located by fixtures, and features on parts. Describing their geometric deviations and interrelationship is essential for variation propagation modeling. These deviations can be defined w.r.t. four types of different coordinate systems (CS).

Definition 1: The *reference coordinate system* (RCS) defines a reference frame in which the physical location and orientation of any element of a MAP can be exactly specified. An RCS coincides with the machine coordinate system of the measuring system, e.g., coordinate-measuring machine.

In this paper, the RCS (marked as $\mathrm{O}_R\mathrm{X}_R\mathrm{Y}_R\mathrm{Z}_R$ in Fig. 2) is assumed to be error free and unchanged for the entire process.

Definition 2: A *fixture coordinate system* (FCS) is rigidly associated with a fixture that locates a part/subassembly. The

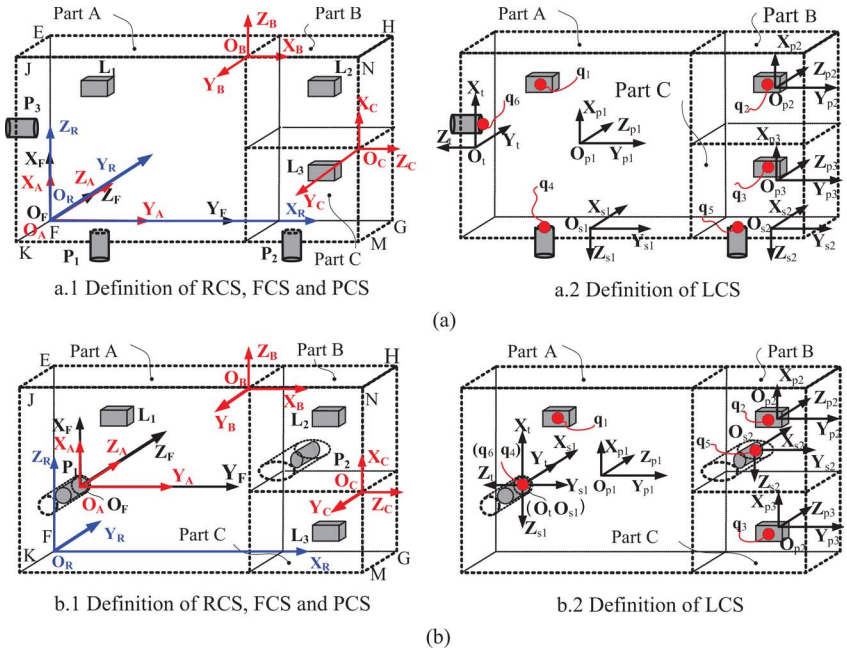

Fig. 2. Illustration of 3-2-1 fixturing scheme and CS definition. (a) General 3-2-1 fixturing scheme. (b) Pin-hole fixturing scheme.

origin of a FCS is at the intersection of the three datum surfaces (or their extensions) of the located part/subassembly. The Z-axis is normal to and pointing from the primary datum (PD) surface and the X-axis is normal to and pointing toward the secondary datum (SD) surface. The Y-axis is normal to and pointing toward the tertiary datum (TD) surface.

Two commonly used 3-2-1 fixturing layouts are considered in this paper. As shown in Fig. 2(a.1), a general 3-2-1 fixturing scheme confines the six degrees of freedom of a subassembly by supporting its PD (EFGH) with three locators L_1, L_2, and L_3, its SD (FKMG) with two locators P_1 and P_2, and its TD (EFKJ) with a locator P_3. A common alternative of it is the pin-hole fixturing scheme, as shown in Fig. 2(b.1). The three locators attaching SD and TD are replaced by a four-way pin P_1 inserted in a hole, and a two-way pin P_2 inserted in a slot. The FCSs (marked as $\mathrm{O}_F\mathrm{X}_F\mathrm{Y}_F\mathrm{Z}_F$ in Fig. 2) of these two layouts are defined accordingly.

Definition 3: A *part coordinate system* (PCS) is rigidly associated with an individual part. The origin of a PCS is at the intersection of the three datum surfaces (or their extensions) of a part. The Z-axis is parallel to the norm of the PD surface and the X-axis is normal to and pointing toward the secondary datum surface. The Y-axis is determined according to the right-hand rule (RHR).

PCS is the foundation that establishes the orientation, alignment, and origin of the part inspection. It provides the frame in which locations and orientations of features are referred. Each individual part is assigned with a unique PCS, such as part A (marked as $\mathrm{O}_\mathrm{A}\mathrm{X}_\mathrm{A}\mathrm{Y}_\mathrm{A}\mathrm{Z}_\mathrm{A}$) in Fig. 2.

Definition 4: A *local coordinate system* (LCS) is rigidly associated with a part feature. The origin of a LCS is the geometric center of a feature. The Z-axis coincides with the norm of the feature surface. The X-axis and the Y-axis are defined in a plane that is perpendicular to the Z-axis, with their positive direction determined according to RHR. For simplicity, these three axes of a LCS can be set to be parallel to that of the corresponding PCS, if applicable.

According to their functional roles in a MAP, part features can be classified into three categories. 1) Datum features or components of datum surfaces, for instance, in Fig. 2(a.2) and (b.2), surface features p1 (denoted as $\mathrm{O}_{\mathrm{p1}}\mathrm{X}_{\mathrm{p1}}\mathrm{Y}_{\mathrm{p1}}\mathrm{Z}_{\mathrm{p1}}$ in Fig. 2), p2 and p3 compose the PD of the subassembly, surface features s1 and s2 compose the SD, and surface feature t serves as the TD. These datum features will induce deviations from upstream assembly stages or part fabrication processes. 2) Matting features, which serve as fixture locators to locate other parts/subassemblies. 3) Measurement features, for instance, features s1 and s2 in Fig. 2(b.2) also serve as the components of a KPC, which is defined as the distance between the center of the hole, s1, and that of the slot, s2. To construct the model, a LCS will be assigned to every feature that serves above two functional roles.

In this paper, a structured notation scheme is defined to denote the four types of CSs. It is considered that a MAP with N stages is used to assemble S parts together to form a product. There is only one RCS for the entire MAP and it is denoted as "R." There are J_k fixtures used at stage $k(k = 1, 2, \ldots, N)$. The nominal FCS of fixture j used at stage k is denoted as "${}^0F_{k,j}$" $(j = 1, 2, \ldots, J_k)$, whereas "$F_{k,j}$" denotes the actual FCS, which may deviate from the nominal one due to the fixture errors. Corresponding to three types of features defined in the paper, there are two types of LCS representation. "$T_{\bullet,k,j}$" $(\bullet \in \{\mathrm{p1}, \mathrm{p2}, \mathrm{p3}, \mathrm{s1}, \mathrm{s2}, \mathrm{t}\})$ denotes the LCS of a feature that serves as the datum feature "$\bullet$" of fixture j at stage k. "$T_{\circ,k,j}$" $(\circ \in \{\mathrm{L}_1, \mathrm{L}_2, \mathrm{L}_3, \mathrm{P}_1, \mathrm{P}_2, \mathrm{P}_3\})$ denotes the LCS of a feature that serves as the fixture locator "$\circ$" of fixture j at stage k. "$T_{*,k,m}$" $(* = 1, 2, \ldots, M_{k,m})$ denotes the LCS of a feature that serves as the $*$th feature involved in calculating the mth KPC measured at stage k. $M_{k,m}$ is the total number of features

involved in calculating the mth KPC at stage k. The PCS of part r ($r = 1, 2, \ldots, S$) is denoted as P_r. The association between features and parts can be identified with an indexing function

$$\text{part index} = i(\text{feature index}). \tag{1}$$

For instance, i ($\bullet$, k, j) gives the index of the part that contains feature "$\bullet$, k, j."

B. Vectorial Deviation Representation

Based on the definitions of CSs, the deviation of an element in a MAP can be represented as the deviation of its actual CS w.r.t. to its own ^{0}CS or another CS, such as a PCS or the RCS. The linear transformation between these CSs can be mathematically represented as a vector [16].

The position and the orientation of an element can be defined by a vector that consists of a location vector and an orientation angular vector w.r.t. a certain CS. For instance, CS_1 can be defined w.r.t. CS_2, as $\mathbf{r}_1^2 = [(\mathbf{t}_1^2)^{\mathrm{T}}(\boldsymbol{\omega}_1^2)^{\mathrm{T}}]^{\mathrm{T}}$, where $\mathbf{t}_1^2 = [x_1^2\ y_1^2\ z_1^2]^{\mathrm{T}}$ and $\boldsymbol{\omega}_1^2 = [\phi_1^2\ \theta_1^2\ \psi_1^2]^{\mathrm{T}}$. This indicates that the projections of O_1 on X_2, Y_2, and Z_2 are x_1^2, y_1^2 and z_1^2, respectively. The orientation of axes X_1, Y_1, and Z_1 can be obtained by sequentially rotating CS_2 around Z_2, Y_2' (after the first rotation) and Z_2'' (after the second rotation) with Euler angles of ϕ_1^2, θ_1^2, and ψ_1^2, respectively. For instance, the Euler angles of part A (CS_1) w.r.t. reference (CS_2) are $\phi_1^2 = -\pi/2$, $\theta_1^2 = -\pi/2$, and $\psi_1^2 = 0$, as shown in Fig. 2(a.1). With this mechanism, the interactions among features, parts and fixtures in a MAP can be described with the geometrical relationships among their CSs, by directly using homogeneous transformation matrix (HTM). Assuming that the vectorial representation of CS_1 w.r.t. CS_2 is $\mathbf{r}_1^2$, the HTM, as a function of $\mathbf{r}_1^2$, is defined as

$$\mathbf{H}(\mathbf{r}_1^2) = \mathbf{H}\left(\begin{bmatrix}\mathbf{t}_1^2\\ \boldsymbol{\omega}_1^2\end{bmatrix}\right) = \begin{bmatrix}\mathbf{R}\left(\boldsymbol{\omega}_1^2\right) & \mathbf{t}_1^2\\ \mathbf{0} & 1\end{bmatrix} \tag{2}$$

where, as shown in (3) at the bottom of the page, is a rotation matrix of the orientation vector, $\boldsymbol{\omega}_1^2$; "c" and "s" denote "cos" function and "sin" function, respectively.

Based on the CS definition, the deviations of the three elements in a MAP can be represented by DMVs [17] defined in their own nominal CSs. For instance, the deviation of CS_1 w.r.t. CS_2 is represented as $\mathbf{x}_1^2 = [(\mathbf{d}_1^2)^{\mathrm{T}}(\boldsymbol{\delta}_1^2)^{\mathrm{T}}]^{\mathrm{T}}$, where $\mathbf{d}_1^2$ contains three small translational deviations ($\Delta\mathrm{X}_1$, $\Delta\mathrm{Y}_1$ and $\Delta\mathrm{Z}_1$) and $\boldsymbol{\delta}_1^2$ contains three small rotational deviations ($\Delta\phi_1$, $\Delta\theta_1$ and $\Delta\psi_1$). Also by using HTM, deviations of a part, e.g., part A, can be mathematically described by $\mathbf{H}(\mathbf{x}_1^2) = \mathbf{H}([(\mathbf{d}_1^2)^{\mathrm{T}}(\boldsymbol{\delta}_1^2)^{\mathrm{T}}]^{\mathrm{T}})$.

In this paper, the induction, transmission and accumulation of deviations are modeled as a series of homogeneous transformations w.r.t. different CSs. These transformations are nonlinear in nature due to the involvement of DMVs. Based on the assumption that magnitudes of DMV elements are small, these nonlinear transformations are linearized by the following lemma (Zhou *et al.* [8]).

Lemma 1: Considering a general transformation between three CSs, CS_1, CS_2, and CS_3, given the coordinate vectors of $\mathbf{r}_2^1$ and $\mathbf{r}_3^2$ and the DMVs of $\mathbf{x}_2^1$ and $\mathbf{x}_3^2$, the DMV of $\mathbf{x}_3^1$ can be derived by using HTM of $\mathbf{H}(\mathbf{r}_2^1)\mathbf{H}(\mathbf{x}_2^1)\mathbf{H}(\mathbf{r}_3^2)\mathbf{H}(\mathbf{x}_3^2)$. By neglecting higher order small values, the transformation can be linearized as

$$\mathbf{x}_3^1 = \mathbf{M}_3^2 \cdot \mathbf{x}_2^1 + \mathbf{x}_3^2 \tag{4}$$

where

$$\mathbf{M}_3^2 = \begin{bmatrix}\left(\mathbf{R}\left(\boldsymbol{\omega}_3^2\right)\right)^{\mathrm{T}} & -\left(\mathbf{R}\left(\boldsymbol{\omega}_3^2\right)\right)^{\mathrm{T}} \cdot \left(\hat{\mathbf{t}}_3^2\right)\\ \mathbf{0} & \left(\mathbf{R}\left(\boldsymbol{\omega}_3^2\right)\right)^{\mathrm{T}}\end{bmatrix}.$$

The skew symmetric matrix $\hat{\mathbf{t}}_3^2$ is determined by the *nominal* location vector $\mathbf{t}_3^2$ ($\mathbf{t}_3^2 = [x_3^2\ y_3^2\ z_3^2]^{\mathrm{T}}$) as

$$\hat{\mathbf{t}}_3^2 = \begin{bmatrix}0 & -z_3^2 & y_3^2\\ z_3^2 & 0 & -x_3^2\\ -y_3^2 & x_3^2 & 0\end{bmatrix}. \tag{5}$$

This transformation can be used to derive the deviation transition among different CSs. For instance, given the deviation of a feature ($\mathrm{T}_{\bullet,k,j}$, CS_3) w.r.t. a part ($P_{i(\bullet,k,j)}$, CS_2), and the deviation of the part w.r.t. reference (R, CS_1), the deviation of the feature w.r.t. reference can be derived from the nominal location and orientation of the $P_{i(\bullet,k,j)}$ in R, as defined in (4).

III. State Space Modeling for MAP

Variation propagation modeling is a procedure of describing the random deviation transition among different CSs. The model coefficients are determined by the part design, process sequences, fixturing schemes and geometric relationships among fixture locators, parts, and features on the parts. The entire modeling can be constructed by three steps: 1) modeling the deviation components, 2) modeling deviation propagation, and 3) modeling deviations of measurements, which will be discussed in the following three subsections.

A. Modeling Deviation Components

At stage k of a MAP, overall dimensional deviations consist of components that are contributed by three types of sources.

1) Assembly Process Induced Deviations: Including the deviations of fixture locators and operation deviations. Operation deviations are caused by the devices performing assembly operation *after* the part/subassembly being located by the fixtures. Thus, this type of deviations is represented as the deviation of a PCS w.r.t. the actual FCS, i.e., $\mathbf{x}_{P_r}^{F_{k,j}}$. As discussed by Camelio

$$\mathbf{R}\left(\boldsymbol{\omega}_1^2\right) = \begin{bmatrix}\mathrm{c}\phi_1^2\mathrm{c}\theta_1^2\mathrm{c}\psi_1^2 - \mathrm{s}\phi_1^2\mathrm{s}\psi_1^2 & -\mathrm{c}\phi_1^2\mathrm{c}\theta_1^2\mathrm{s}\psi_1^2 - \mathrm{s}\phi_1^2\mathrm{c}\psi_1^2 & \mathrm{c}\phi_1^2\mathrm{s}\theta_1^2\\ \mathrm{s}\phi_1^2\mathrm{c}\theta_1^2\mathrm{c}\psi_1^2 + \mathrm{c}\phi_1^2\mathrm{s}\psi_1^2 & -\mathrm{s}\phi_1^2\mathrm{c}\theta_1^2\mathrm{s}\psi_1^2 + \mathrm{c}\phi_1^2\mathrm{c}\psi_1^2 & \mathrm{s}\phi_1^2\mathrm{s}\theta_1^2\\ -\mathrm{s}\theta_1^2\mathrm{c}\psi_1^2 & \mathrm{s}\theta_1^2\mathrm{s}\psi_1^2 & \mathrm{c}\theta_1^2\end{bmatrix} \tag{3}$$

et al. [18], operation deviation is a composition of many possible deviation sources, which are quite dependent on particular operation situation. Detailed modeling of certain types of operations has been thoroughly studied at single-stage level in [19]–[21]. To simplify the problem and focus on the variation propagation modeling of rigid body assembly processes, this paper assumes that the operation deviations are given as modeling inputs.

It is considered that there are J_k fixtures used at stage k to locate J_k parts/subassemblies. Each fixture, as illustrated in Fig. 2(a), is made up of six fixture locators. The coordinates of L_h in ${}^0F_{k,j}$ are $(L_{hx}^{{}^0F_{k,j}}, L_{hy}^{{}^0F_{k,j}}, L_{hz}^{{}^0F_{k,j}})$, $h = 1,2,3$, and that of P_w are $(P_{wx}^{{}^0F_{k,j}}, P_{wy}^{{}^0F_{k,j}}, P_{wz}^{{}^0F_{k,j}})$, where $w = 1,2,3$. For the fixture scheme in Fig. 2(b), five locators are used and can be described with a similar format. According to the fundamental requirement on deterministic localization, parts/subassembly datum surfaces must be in contact with fixture locators at locating points. This means that the deviation of the parts/subassembly is equivalent to that of the fixture and can be described by the kinematics of the fixture system. Thus, fixture induced deviations are represented as the deviation of $F_{k,j}$ w.r.t. ${}^0F_{k,j}$, i.e., $\mathbf{x}_{F_{k,j}}^{{}^0F_{k,j}}$. These deviations are caused by small deviations of fixture locators, denoted as

$$\mathbf{u}_{k,j}^{{}^0F_{k,j}} = \left[\Delta L_{1z}^{{}^0F_{k,j}} \Delta L_{2z}^{{}^0F_{k,j}} \Delta L_{3z}^{{}^0F_{k,j}} \Delta P_{1x}^{{}^0F_{k,j}} \Delta P_{2x}^{{}^0F_{k,j}} \Delta P_{3y}^{{}^0F_{k,j}}\right]^{\mathrm{T}}. \tag{6}$$

Analytical research has been conducted by Cai *et al.* [22] to study the infinitesimal error of rigid body fixturing scheme. Based on their results and the fixture error analysis strategy in [8], fixture induced deviation is modeled as a linear transformation of the fixture locator deviations

$$\mathbf{x}_{F_{k,j}}^{{}^0F_{k,j}} = \mathbf{T}_{k,j} \cdot \mathbf{u}_{k,j}^{{}^0F_{k,j}} \tag{7}$$

where the coefficient matrix $\mathbf{T}_{k,j}$ is derived according to the geometric configuration of the fixture, i.e., coordinates of the six locators. It completely characterizes the kinematics of a fixture system. The matrices $\mathbf{T}_{k,j}$ under two different fixturing schemes are given in Appendix I.

In a generic Type I assembly process, it is not unusual to use matting features on some parts as fixture locators to locate other parts. In such cases, $\mathbf{u}_{k,j}^{{}^0F_{k,j}}$ in (7) should be derived from the deviations of matting features w.r.t. ${}^0\mathrm{FCS}$.

Lemma 2: If the function of fixture j at stage k is implemented by matting features, the deviations of fixture locators can be derived as

$$\mathbf{u}_{k,j}^{{}^0F} = \mathbf{S}_{k,j}^0 \left(\mathbf{G}_{k,j} {}^L\mathbf{x}_{k,j}^R + {}^L\mathbf{x}_{k,j}\right) \tag{8}$$

where $\mathbf{S}_{k,j}^0$ is a selector matrix, i.e., $\mathbf{S}_{k,j}^0 = \mathrm{diag}\{\mathbf{s}_\circ(\eta)\}$, $\circ \in \{\mathrm{L}_1, \mathrm{L}_2, \mathrm{L}_3, \mathrm{P}_1, \mathrm{P}_2, \mathrm{P}_3\}$ and $\mathbf{s}_\circ(\eta)$ is an 1×6 vector with the ηth element equal to 1 and others equal to 0; ${}^L\mathbf{x}_{k,j} = [(\mathbf{x}_{T_{L_1,k,j}}^{P_{i(L_1,k,j)}})^{\mathrm{T}} \ (\mathbf{x}_{T_{L_2,k,j}}^{P_{i(L_2,k,j)}})^{\mathrm{T}} \ (\mathbf{x}_{T_{L_3,k,j}}^{P_{i(L_3,k,j)}})^{\mathrm{T}} \ (\mathbf{x}_{T_{P_1,k,j}}^{P_{i(P_1,k,j)}})^{\mathrm{T}} \ (\mathbf{x}_{T_{P_2,k,j}}^{P_{i(P_2,k,j)}})^{\mathrm{T}} \ (\mathbf{x}_{T_{P_3,k,j}}^{P_{i(P_3,k,j)}})^{\mathrm{T}}]^{\mathrm{T}}$ is a stack-up of DMVs of the six matting features w.r.t. the PCSs of the parts that contains them; ${}^L\mathbf{x}_{k,j}^R = [(\mathbf{x}_{P_{i(L_1,k,j)}}^R)^{\mathrm{T}} \ (\mathbf{x}_{P_{i(L_2,k,j)}}^R)^{\mathrm{T}} \ (\mathbf{x}_{P_{i(L_3,k,j)}}^R)^{\mathrm{T}} \ (\mathbf{x}_{P_{i(P_1,k,j)}}^R)^{\mathrm{T}} (\mathbf{x}_{P_{i(P_2,k,j)}}^R)^{\mathrm{T}} \ (\mathbf{x}_{P_{i(P_3,k,j)}}^R)^{\mathrm{T}}]^{\mathrm{T}}$ is a stack-up of the DMVs of the six parts w.r.t. RCS. $\mathbf{G}_{k,j}$ is a diagonal block matrix, i.e.,

$$\mathbf{G}_{k,j} = \mathrm{diag}\left\{\mathbf{M}_{T_{\circ,k,j}}^{P_{i(\circ,k,j)}}\right\}. \tag{9}$$

Proof: Given the DMV of a matting feature w.r.t. the PCS of the part that contains it, $\mathbf{x}_{T_{\circ,k,j}}^{P_{i(\circ,k,j)}} (\circ \in \{\mathrm{L}_1, \mathrm{L}_2, \mathrm{L}_3, \mathrm{P}_1, \mathrm{P}_2, \mathrm{P}_3\})$, and the DMV of a PCS w.r.t. the RCS, $\mathbf{x}_{P_{i(\circ,k,j)}}^R$, the DMV of that matting feature w.r.t. the RCS can be derived by applying Lemma 1, i.e., $\mathbf{x}_{T_{\circ,k,j}}^R = \mathbf{M}_{T_{\circ,k,j}}^{P_{i(\circ,k,j)}} \cdot \mathbf{x}_{P_{i(\circ,k,j)}}^R + \mathbf{x}_{T_{\circ,k,j}}^{P_{i(\circ,k,j)}}$. The DMV of that matting feature w.r.t. the nominal FCS can be further derived by applying Lemma 1, i.e., $\mathbf{x}_{T_{\circ,k,j}}^{{}^0F_{k,j}} = \mathbf{M}_{T_{\circ,k,j}}^R \mathbf{x}_R^{{}^0F_{k,j}} + \mathbf{x}_{T_{\circ,k,j}}^R$. It is rational to assume that ${}^0F_{k,j}$ has no deviation w.r.t. RCS, i.e., DMV $\mathbf{x}_{{}^0F_{k,j}}^R = \mathbf{x}_R^{{}^0F_{k,j}} = \mathbf{0}$, thus

$$\mathbf{x}_{T_{\circ,k,j}}^{{}^0F_{k,j}} = \mathbf{x}_{T_{\circ,k,j}}^R = \mathbf{M}_{T_{\circ,k,j}}^{P_{i(\circ,k,j)}} \cdot \mathbf{x}_{P_{i(\circ,k,j)}}^R + \mathbf{x}_{T_{\circ,k,j}}^{P_{i(\circ,k,j)}}. \tag{10}$$

For each matting feature, only the deviation along one direction will cause the deviation of the fixture system. Thus, an 1×6 selector vector $\mathbf{s}_\circ(\eta)$ is used to select the particular directional deviation from $\mathbf{x}_{T_{\circ,k,j}}^{{}^0F_{k,j}}$. For instance, $\Delta L_{1z}^{{}^0F_{k,j}}$ is obtained from the third element of $\mathbf{x}_{T_{L_1,k,j}}^{{}^0F_{k,j}}$, i.e., $\Delta L_{1z}^{{}^0F_{k,j}} = \mathbf{s}_{L_1}(3) \cdot \mathbf{x}_{T_{L_1,k,j}}^{{}^0F_{k,j}}$. There are six matting features serving as fixture locators. Thus, it is straightforward to stack up (10) and the selector vector $\mathbf{s}_\circ(\eta)$ to get (8).

2) Datum Features Induced Deviations: Including the datum features deviations modeled as the deviations of the actual FCS w.r.t. the RCS, which are caused by preceding assembly processes [or called reorientation induced deviation [6], as the deviation of subassembly BC shown in Fig. 3(b)], and that caused by the part fabrication processes [as the deviation of slot feature on part A in Fig. 3(b)]. □

The datum scheme corresponding to a general 3-2-1 fixture j at stage k is illustrated in Fig. 2(a). The PD is composed of three features: $p_{1,k,j}$, $p_{2,k,j}$, and $p_{3,k,j}$, which are in touch with locators L_1, L_2 and L_3 at datum points q_1, q_2, and q_3, respectively. The SD consists of two features, $s_{1,k,j}$ and $s_{2,k,j}$, touching locators P_1 and P_2 at datum points q_4 and q_5, respectively. The TD is denoted as $t_{k,j}$, which touches locator P_3 at datum point q_6. Therefore, the datum feature induced deviation can be modeled as the deviation of the actual FCS w.r.t. the RCS, which is given by Lemma 3.

Lemma 3: For fixture j at stage k, given the DMVs of the six datum features w.r.t. RCS, $\mathbf{x}_{T_{p_1,k,j}}^R$, $\mathbf{x}_{T_{p_2,k,j}}^R$, $\mathbf{x}_{T_{p_3,k,j}}^R$, $\mathbf{x}_{T_{s_1,k,j}}^R$, $\mathbf{x}_{T_{s_2,k,j}}^R$, and $\mathbf{x}_{T_{t,k,j}}^R$, datum induced deviations are modeled as the deviations of $F_{k,j}$ w.r.t. R, and can be derived as

$$\begin{aligned}\mathbf{x}_{F_{k,j}}^R = {} & \mathbf{T}_{1,k,j}\mathbf{x}_{T_{p_1,k,j}}^R + \mathbf{T}_{2,k,j}\mathbf{x}_{T_{p_2,k,j}}^R + \mathbf{T}_{3,k,j}\mathbf{x}_{T_{p_3,k,j}}^R \\ & + \mathbf{T}_{4,k,j}\mathbf{x}_{T_{s_1,k,j}}^R + \mathbf{T}_{5,k,j}\mathbf{x}_{T_{s_2,k,j}}^R + \mathbf{T}_{6,k,j}\mathbf{x}_{T_{t,k,j}}^R\end{aligned} \tag{11}$$

where $T_{1,k,j}$ through $T_{6,k,j}$ are determined by the nominal location of the six datum points, q_1 through q_6, and that of fixture locators, as shown in Fig. 2(a.2). The derivation procedure of $\mathbf{T}_{1,k,j}$ through $\mathbf{T}_{6,k,j}$ can be found in Appendix II.

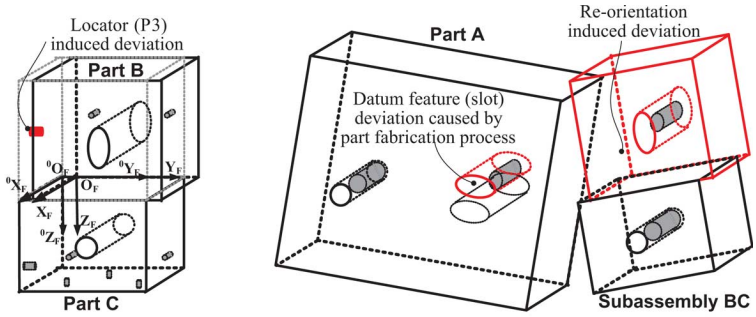

(a) Process induced deviation at stage 1 (b) Datum induced deviation at stage 2

Fig. 3. Illustration of deviation sources in a MAP.

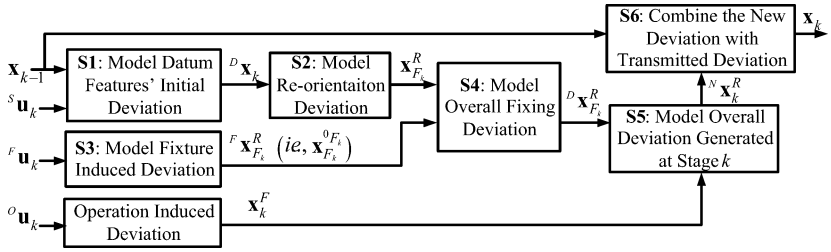

Fig. 4. Procedure of derivation of deviation propagation model.

3) Noises: Including the system noise that cannot be modeled with the linear state space representation and the noises introduced by measurement devises.

B. Modeling Deviation Propagation

Based on the geometric deviation representation of three elements in a MAP, and the modeling of deviation components that induced by datum features and fixture locators, variation propagation can be described in a state space model. As denoted in Fig. 1, the deviation of an assembly after stage k is represented by a state vector $\mathbf{x}_k$, which is a stack-up of the DMVs of all parts assembled. With the deviation of part $r(r = 1, 2, \ldots, S)$ at stage k being represented as a 6×1 DMV, $\mathbf{x}^R_{k,r}$, the state vector of S parts will be $\mathbf{x}_k = [(\mathbf{x}^R_{k,1})^{\mathrm{T}}(\mathbf{x}^R_{k,2})^{\mathrm{T}} \cdots (\mathbf{x}^R_{k,S})^{\mathrm{T}}]^{\mathrm{T}}$. It is the DMVs of parts, not that of features, that compose a state vector. Thus, the dimension of a state vector will only be determined by the number of parts in a MAP, i.e., $6S \times 1$, no matter how many features are considered. This strategy prevents the dimension of state vectors from significantly growing when a large system is modeled. Before the first stage, there is no process operated and therefore no deviations, i.e., $\mathbf{x}_0 = \mathbf{0}_{6S\times 1}$. As parts or subassemblies passing through a MAP, the elements of $\mathbf{x}_k$ corresponding to the assembled parts may be changed to reflect their quality deviations, whereas those elements corresponding to unassembled parts remain zeros.

Denoting $\mathbf{x}_{k-1}$ as the state vector after stage $k-1$, all deviations induced by part fabrication processes and the assembly process performed at stage k as $\mathbf{u}_k$, and deviations of in-process KPCs measured at stage k as $\mathbf{y}_k$, the variation propagation in a MAP can be formulated in a linear discrete state space model

$$\begin{aligned} \mathbf{x}_k &= \mathbf{A}_k\mathbf{x}_{k-1} + \mathbf{B}_k\mathbf{u}_k + \mathbf{w}_k \\ \mathbf{y}_k &= \mathbf{C}_k\mathbf{x}_k + \mathbf{D}_k\mathbf{u}_k + \mathbf{v}_k \end{aligned} \tag{12}$$

where $\mathbf{A}_k\mathbf{x}_{k-1}$ represents the deviations transmitted from upstream stages by reorientation movements; $\mathbf{B}_k\mathbf{u}_k$ represents the deviations introduced from stage k; $\mathbf{C}_k\mathbf{x}_k$ reflects that the KPC deviations are calculated from the linear combination of $\mathbf{x}_k$; the KPC deviations contributed by the part fabrication processes are captured by $\mathbf{D}_k\mathbf{u}_k$; $\mathbf{w}_k$ and $\mathbf{v}_k$ are the unmodeled system noise and measurement noise, respectively.

Lemma 3 and (7) provide the basis for modeling deviation propagation at a multistage level. It is a procedure of deriving system matrices in the state transition equation of (12). Fig. 4 shows six major steps of deriving the system matrices $\mathbf{A}_k$ and $\mathbf{B}_k$, which are discussed in details as follows.

S1 Modeling initial deviations of datum features. For a part/subassembly located at stage k, the initial deviations of datum features can be derived by the following lemma.

Lemma 4: For a part/subassembly located by fixture j at stage k, the initial deviations of datum features are represented as the DMVs of features w.r.t. the RCS, and can be derived as

$${}^{D}\mathbf{x}^R_{k,j} = \mathbf{A}^1_{k,j} \cdot \mathbf{S}^1_{k,j} \cdot \mathbf{x}_{k-1} + {}^{S}\mathbf{x}_{k,j} \tag{13}$$

where ${}^{D}\mathbf{x}^R_{k,j} = [(\mathbf{x}^R_{T_{p1},k,j})^{\mathrm{T}}(\mathbf{x}^R_{T_{p2},k,j})^{\mathrm{T}}(\mathbf{x}^R_{T_{p3},k,j})^{\mathrm{T}}\ (\mathbf{x}^R_{T_{s1},k,j})^{\mathrm{T}}\ (\mathbf{x}^R_{T_{s2},k,j})^{\mathrm{T}}(\mathbf{x}^R_{T_{t},k,j})^{\mathrm{T}}]^{\mathrm{T}}$; $\mathbf{A}^1_{k,j} = \mathrm{diag}\{\mathbf{M}^{P_{i(\bullet,k,j)}}_{T_{\bullet},k,j}\}$, $\bullet \in \{\mathrm{p1}, \mathrm{p2}, \mathrm{p3}, \mathrm{s1}, \mathrm{s2}, \mathrm{t}\}$, is a diagonal block matrix with six diagonal blocks $\mathbf{M}^{P_{i(\bullet,k,j)}}_{T_{\bullet},k,j}$; the selector matrix $\mathbf{S}^1_{k,j}$ is determined by the datum scheme defined in the process design, and

$$\mathbf{S}^1_{k,j} = \left[\boldsymbol{\theta}^{\mathrm{T}}_{i(p1,k,j)}\boldsymbol{\theta}^{\mathrm{T}}_{i(p2,k,j)}\boldsymbol{\theta}^{\mathrm{T}}_{i(p3,k,j)}\boldsymbol{\theta}^{\mathrm{T}}_{i(s1,k,j)}\boldsymbol{\theta}^{\mathrm{T}}_{i(s2,k,j)}\boldsymbol{\theta}^{\mathrm{T}}_{i(t,k,j)}\right]^{\mathrm{T}} \tag{14}$$

where $\boldsymbol{\theta}_{i(\bullet,k,j)}$ is a 6×6 S matrix consisting of S submatrices with the dimension of 6×6, and the $i(\bullet, k, j)$th submatrix is an identity matrix and others are zero matrices; $\mathbf{x}_{k-1}$ is the state vector of stage

$k-1$; ${}^{S}\mathbf{x}_{k,j} = [(\mathbf{x}_{T_{p1},k,j}^{P_{i(p1,k,j)}})^{\mathrm{T}}(\mathbf{x}_{T_{p2},k,j}^{P_{i(p2,k,j)}})^{\mathrm{T}}(\mathbf{x}_{T_{p3},k,j}^{P_{i(p3,k,j)}})^{\mathrm{T}}(\mathbf{x}_{T_{s1},k,j}^{P_{i(s1,k,j)}})^{\mathrm{T}}(\mathbf{x}_{T_{s2},k,j}^{P_{i(s2,k,j)}})^{\mathrm{T}}(\mathbf{x}_{T_{t},k,j}^{P_{i(t,k,j)}})^{\mathrm{T}}]^{\mathrm{T}}$.

Proof: Given the DMV of a datum feature w.r.t. the PCS of the part that contains it, $\mathbf{x}_{T_{\bullet},k,j}^{P_{i(\bullet,k,j)}}(\bullet \in \{\mathrm{p1},\mathrm{p2},\mathrm{p3},\mathrm{s1},\mathrm{s2},\mathrm{t}\})$, and the DMV of the PCS w.r.t. RCS, $\mathbf{x}_{P_{i(\bullet,k,j)}}^{R}$, the DMV of the datum feature w.r.t. RCS can be derived by applying Lemma 1, i.e.,

$$\mathbf{x}_{T_{\bullet},k,j}^{R} = \mathbf{M}_{T_{\bullet},k,j}^{P_{i(\bullet,k,j)}} \cdot \mathbf{x}_{P_{i(\bullet,k,j)}}^{R} + \mathbf{x}_{T_{\bullet},k,j}^{P_{i(\bullet,k,j)}}. \tag{15}$$

The deviation of the PCS is transmitted from stage $k-1$; thus, $\mathbf{x}_{P_{i(\bullet,k,j)}}^{R}$ is selected from $\mathbf{x}_{k-1}$, i.e.,

$$\mathbf{x}_{P_{i(\bullet,k,j)}}^{R} = \boldsymbol{\theta}_{i(\bullet,k,j)}\mathbf{x}_{k-1}. \tag{16}$$

There are six datum features involved with fixture j at stage k. Thus, it is straightforward to stack up $\mathbf{M}_{T_{\bullet},k,j}^{P_{i(\bullet,k,j)}}$ in (15) to form diagonal matrix $\mathbf{A}_{k,j}^{1}$, and to stack up $\boldsymbol{\theta}_{i(\bullet,k,j)}$ in (16) to form the selector matrix $\mathbf{S}_{k,j}^{1}$.

Lemma 4 indicates that the initial deviations of datum features are contributed by two sources: the part deviations generated at the preceding stages and that generated when the incoming parts are fabricated. The initial deviations of datum features modeled by (13) can be expanded to all J_k fixtures used at stage k.

Corollary 4.1: The initial deviations of datum features corresponding to all J_k fixtures can be derived as

$${}^{D}\mathbf{x}_{k} = \mathbf{A}_{k}^{1} \cdot \mathbf{A}_{k}^{0} \cdot \mathbf{x}_{k-1} + {}^{S}\mathbf{u}_{k} \tag{17}$$

where ${}^{D}\mathbf{x}_{k} = [({}^{D}\mathbf{x}_{k,1}^{R})^{\mathrm{T}}({}^{D}\mathbf{x}_{k,2}^{R})^{\mathrm{T}},\ldots,({}^{D}\mathbf{x}_{k,J_k}^{R})^{\mathrm{T}}]^{\mathrm{T}}$, $\mathbf{A}_{k}^{0} = [(\mathbf{S}_{k,1}^{1})^{\mathrm{T}}\ (\mathbf{S}_{k,2}^{1})^{\mathrm{T}},\ldots,(\mathbf{S}_{k,J_k}^{1})^{\mathrm{T}}]^{\mathrm{T}}$, $\mathbf{A}_{k}^{1} = \mathrm{diag}\left\{\mathbf{A}_{k,j}^{1}\right\}, j = 1,2,\ldots,J_k$, ${}^{S}\mathbf{u}_{k} = [({}^{S}\mathbf{x}_{k,1})^{\mathrm{T}}({}^{S}\mathbf{x}_{k,2})^{\mathrm{T}},\ldots,({}^{S}\mathbf{x}_{k,J_k})^{\mathrm{T}}]^{\mathrm{T}}$.

Please note that in (17), ${}^{D}\mathbf{x}_{k} \in \Re^{36\cdot J_k\times 1}$, ${}^{S}\mathbf{u}_{k} \in \Re^{36\cdot J_k\times 1}$, and $\mathbf{A}_{k}(1) \in \Re^{36J_k\times 36J_k}$.

S2 Modeling reorientation deviations. The reorientation deviations are caused by the initial deviations of datum features. These deviations can be derived by substituting ${}^{D}\mathbf{x}_{k,j}^{R}$ in (13) for that in (11).

Lemma 5: For fixture j at stage k, the reorientation deviations are modeled by DMV of $F_{k,j}$ w.r.t. R, and can be derived as

$${}^{D}\mathbf{x}_{F_{k,j}}^{R} = \mathbf{A}_{k,j}^{2} \cdot {}^{D}\mathbf{x}_{k,j}^{R} \tag{18}$$

where $\mathbf{A}_{k,j}^{2} = [\mathbf{T}_{1,k,j}\mathbf{T}_{2,k,j}\mathbf{T}_{3,k,j}\mathbf{T}_{4,k,j}\mathbf{T}_{5,k,j}\mathbf{T}_{6,k,j}]$ for general 3-2-1 fixturing scheme, or $\mathbf{A}_{k,j}^{2} = [\mathbf{T}_{1,k,j}\mathbf{T}_{2,k,j}\mathbf{T}_{3,k,j}\mathbf{T}_{4,k,j}^{*}\mathbf{T}_{5,k,j}^{*}\mathbf{T}_{6,k,j}^{*}]$ for the pin-hole fixturing scheme.

Corollary 5.1: The datum induced reorientation deviations for all J_k fixtures at stage k are

$${}^{D}\mathbf{x}_{F_k}^{R} = \mathbf{A}_{k}^{2} \cdot {}^{D}\mathbf{x}_{k} \tag{19}$$

where ${}^{D}\mathbf{x}_{F_k}^{R} = [({}^{D}\mathbf{x}_{F_{k,1}}^{R})^{\mathrm{T}}({}^{D}\mathbf{x}_{F_{k,2}}^{R})^{\mathrm{T}},\ldots,({}^{D}\mathbf{x}_{F_{k,J_k}}^{R})^{\mathrm{T}}]^{\mathrm{T}}$, $\mathbf{A}_{k}^{2} = \mathrm{diag}\left\{\mathbf{A}_{k,j}^{2}\right\}, j = 1,2,\ldots,J_k$, and $\mathbf{A}_{k}^{2} \in \Re^{6\cdot J_k\times 6\cdot J_k}$.

S3 Modeling fixture induced deviations. The fixture induced deviations are caused by the deviations of fixture locators.

Lemma 6: For fixture j at stage k, fixture induced deviations are modeled by DMV of $F_{k,j}$ w.r.t. R, and can be derived as

$${}^{F}\mathbf{x}_{F_{k,j}}^{R} = \mathbf{A}_{k,j}^{3} \cdot {}^{0F}\mathbf{u}_{k,j}^{F} \tag{20}$$

where $\mathbf{A}_{k,j}^{3} = \mathbf{T}_{k,j}$.

Proof: For fixture j at stage k, the DMV of $F_{k,j}$ w.r.t. ${}^{0}F_{k,j}$ can be derived by substituting ${}^{0F}\mathbf{u}_{k,j}^{F}$ in (6) or (8) for that in(7). The DMV of $F_{k,j}$ w.r.t. R can be achieved by applying Lemma 1, i.e., ${}^{F}\mathbf{x}_{F_{k,j}}^{R} = \mathbf{M}_{F_{k,j}}^{{}^{0}F_{k,j}}\mathbf{x}_{{}^{0}F_{k,j}}^{R} + \mathbf{x}_{F_{k,j}}^{{}^{0}F_{k,j}}$. In this paper, ${}^{0}F_{k,j}$ are assumed to be deviation-free, i.e., $\mathbf{x}_{{}^{0}F_{k,j}}^{R} = \mathbf{0}$. Thus, we have ${}^{F}\mathbf{x}_{F_{k,j}}^{R} = \mathbf{x}_{F_{k,j}}^{{}^{0}F_{k,j}} = \mathbf{T}_{k,j} \cdot {}^{0F}\mathbf{u}_{k,j}^{F}$.

This lemma can be expanded to all J_k fixtures at stage k.

Corollary 6.1: The fixture induced deviations for all J_k fixtures at stage k are

$${}^{F}\mathbf{x}_{F_k}^{R} = \mathbf{A}_{k}^{3} \cdot {}^{F}\mathbf{u}_{k} \tag{21}$$

where ${}^{F}\mathbf{x}_{F_k}^{R} = [({}^{F}\mathbf{x}_{F_{k,1}}^{R})^{\mathrm{T}}({}^{F}\mathbf{x}_{F_{k,2}}^{R})^{\mathrm{T}},\ldots,({}^{F}\mathbf{x}_{F_{k,J_k}}^{R})^{\mathrm{T}}]^{\mathrm{T}}$, ${}^{F}\mathbf{u}_{k} = [(\mathbf{u}_{k,1}^{{}^{0}F})^{\mathrm{T}}(\mathbf{u}_{k,2}^{{}^{0}F})^{\mathrm{T}},\ldots,(\mathbf{u}_{k,J_k}^{{}^{0}F})^{\mathrm{T}}]^{\mathrm{T}}$, and $\mathbf{A}_{k}^{3} = \mathrm{diag}\{\mathbf{A}_{k,j}^{3}\}, j = 1,2,\ldots,J_k$. Please note that ${}^{F}\mathbf{u}_{k} \in \Re^{6\cdot J_k\times 1}$ and $\mathbf{A}_{k}^{3} \in \Re^{6\cdot J_k\times 6\cdot J_k}$.

S4 Modeling overall fixturing deviations. The overall fixturing deviations are caused by both the datum induced deviations and the fixture induced deviations, and can be derived by applying Lemma 5, Lemma 6, and their corollaries.

Lemma 7: The overall fixturing deviations of J_k fixtures at stage k are modeled as J_k DMVs of $F_{k,j}$ w.r.t. R and can be derived as

$$\mathbf{x}_{F_k}^{R} = {}^{D}\mathbf{x}_{F_k}^{R} + {}^{F}\mathbf{x}_{F_k}^{R} \tag{22}$$

where $\mathbf{x}_{F_k}^{R} = [(\mathbf{x}_{F_{k,1}}^{R})^{\mathrm{T}}(\mathbf{x}_{F_{k,2}}^{R})^{\mathrm{T}}\ldots(\mathbf{x}_{F_{k,J_k}}^{R})^{\mathrm{T}}]^{\mathrm{T}}$. Please note that $\mathbf{x}_{F_k}^{R}, {}^{D}\mathbf{x}_{F_k}^{R}, {}^{F}\mathbf{x}_{F_k}^{R} \in \Re^{6\cdot J_k\times 1}$.

S5 Calculate overall deviations at stage k. The overall deviations at stage k are the combination of the overall fixturing deviations and the operation deviations.

Lemma 8: It is assumed that there are $l_{k,j}$ parts forming a subassembly, which is located by fixture j at stage k. Please note that if there is only one part located by this fixture, then $l_{k,j} = 1$. The overall deviations are modeled as the DMVs of all $l_{k,j}$ parts w.r.t. R, and can be derived as

$${}^{N}\mathbf{x}_{k,j}^{R} = \mathbf{A}_{k,j}^{4} \cdot \mathbf{x}_{F_{k,j}}^{R} + {}^{O}\mathbf{u}_{k,j} \tag{23}$$

where ${}^{N}\mathbf{x}_{k,j}^{R} = [\mathbf{0}^{\mathrm{T}},\ldots,(\mathbf{x}_{P_{r(1,k,j)}}^{R})^{\mathrm{T}},\ldots,(\mathbf{x}_{P_{r(c,k,j)}}^{R})^{\mathrm{T}}\ldots(\mathbf{x}_{P_{r(l_{k,j},k,j)}}^{R})^{\mathrm{T}},\ldots,\mathbf{0}^{\mathrm{T}}]^{\mathrm{T}}$, ${}^{O}\mathbf{u}_{k,j} = [\mathbf{0}^{\mathrm{T}},\ldots,(\mathbf{x}_{P_{r(1,k,j)}}^{F_{k,j}})^{\mathrm{T}},\ldots,(\mathbf{x}_{P_{r(c,k,j)}}^{F_{k,j}})^{\mathrm{T}}\ldots(\mathbf{x}_{P_{r(l_{k,j},k,j)}}^{F_{k,j}})^{\mathrm{T}},\ldots,\mathbf{0}^{\mathrm{T}}]^{\mathrm{T}}$, $\mathbf{0}$ is a 6×1 vector of zeros; $\mathbf{A}_{k,j}^{4} = [\boldsymbol{\Theta}^{\mathrm{T}},\ldots,(\mathbf{M}_{P_{r(1,k,j)}}^{{}^{0}F_{k,j}})^{\mathrm{T}},\ldots,(\mathbf{M}_{P_{r(c,k,j)}}^{{}^{0}F_{k,j}})^{\mathrm{T}}\ldots(\mathbf{M}_{P_{r(l_{k,j},k,j)}}^{{}^{0}F_{k,j}})^{\mathrm{T}},\ldots,\boldsymbol{\Theta}^{\mathrm{T}}]^{\mathrm{T}}$, and$\boldsymbol{\Theta}$ is a 6×6 matrix of zeros. The subscript $r(c,k,j)$ is a function indicating the index of a part which is the cth part on the subassembly located by fixture j at stage $k, c = 1,2,\ldots,l_{k,j}$, and $r(c,k,j) \in \{1,2,\ldots,S\}$.

Proof: For the part $r(c,k,j)$ that belongs to the subassembly located by fixture j at stage k, the overall deviations

are modeled as the DMV of $P_{r(c,k,j)}$ w.r.t. R. Given the overall fixturing deviations, $\mathbf{x}^R_{F_{k,j}}$, and operation deviations, $\mathbf{x}^{F_{k,j}}_{P_{r(c,k,j)}}$, $\mathbf{x}^R_{P_{r(c,k,j)}}$ can be derived by applying Lemma 1, as

$$\mathbf{x}^R_{P_{r(c,k,j)}} = \mathbf{M}^{F_{k,j}}_{P_{r(c,k,j)}} \cdot \mathbf{x}^R_{F_{k,j}} + \mathbf{x}^{F_{k,j}}_{P_{r(c,k,j)}}. \tag{24}$$

Assuming that deviations of $F_{k,j}$ from ${}^0F_{k,j}$ are very small, according to Zhou *et al.* [8], $\mathbf{M}^{F_{k,j}}_{P_{r(c,k,j)}}$ can be replaced by $\mathbf{M}^{{}^0F_{k,j}}_{P_{r(c,k,j)}}$, which is obtained from process design information. It is straightforward to stack up the components in (24) to form ${}^N\mathbf{x}^R_{k,j}$, $\mathbf{x}^R_{F_{k,j}}$, ${}^O\mathbf{u}_{k,j}$, and $\mathbf{A}^4_{k,j}$ in (23).

The overall deviations corresponding to a single fixture j at stage k is modeled by (23). These overall deviations are the summation of ${}^N\mathbf{x}^R_{k,j}, j = 1, 2, \ldots, J_k$.

Corollary 8.1: The overall deviations for all J_k fixtures at stage k are

$${}^N\mathbf{x}^R_k = \mathbf{A}^4_k \cdot \mathbf{x}^R_{F_k} + {}^O\mathbf{u}_k \tag{25}$$

where ${}^N\mathbf{x}^R_k = \sum_{j=1}^{J_k} \left({}^N\mathbf{x}^R_{k,j}\right)$, $\mathbf{A}^4_k = [\mathbf{A}^4_{k,1}\mathbf{A}^4_{k,2}, \ldots, \mathbf{A}^4_{k,J_k}]$, ${}^O\mathbf{u}_k = \sum_{j=1}^{J_k} {}^O\mathbf{u}_{k,j}$. Please note that ${}^N\mathbf{x}^R_k$ and ${}^O\mathbf{u}_k \in \Re^{6S\times 1}$ and $\mathbf{A}^4_k \in \Re^{6S\times 6FX_k}$.

S6 Calculate overall deviations after stage k. After assembly operations at stage k, the deviations of parts w.r.t. RCS are the combinations of the deviations transmitted from preceding stages and that generated at the current stage k, i.e.,

$$\mathbf{x}_k = \mathbf{x}_{k-1} + {}^N\mathbf{x}^R_k. \tag{26}$$

The intermediate results listed in (13)–(25) are the building-blocks of the system matrices in model (12). Substituting them for ${}^N\mathbf{x}^R_k$ in (26), the state transition equation in model (12) can be represented as

$$\begin{aligned}\mathbf{x}_k = {} & [\mathbf{I}_{6S\times 6S} + \mathbf{A}^4_k \cdot \mathbf{A}^2_k \cdot \mathbf{A}^1_k \cdot \mathbf{A}^0_k]\mathbf{x}_{k-1} \\ & + [\,\mathbf{A}^4_k \cdot \mathbf{A}^2_k \quad \mathbf{A}^4_k \cdot \mathbf{A}^3_k \quad \mathbf{I}_{6S\times 6S}\,] \cdot \begin{bmatrix} {}^S\mathbf{u}_k \\ {}^F\mathbf{u}_k \\ {}^O\mathbf{u}_k \end{bmatrix}\end{aligned} \tag{27}$$

where $\mathbf{I}_{6S\times 6S}$ is a $6S \times 6S$ identity matrix. The detailed derivation is presented in Appendix III.

C. Modeling Deviation Measurements

The observation equation can be derived in a similar way. A KPC, denoted as $y_{k,m}$, is a dimensional deviation relating multiple features on different parts. The linearization of their relationships can be achieved with the method introduced by Cai [23]. In this paper, KPC measurements can be derived by the following lemma.

Lemma 9: Consider that the mth KPC measured at stage k involves $M_{k,m}$ features on different parts, it can be derived that

$$y_{m,k} = \mathbf{c}_{k,m}(\mathbf{C}^1_{k,m} \cdot \mathbf{S}^2_{k,m} \cdot \mathbf{x}_k + {}^M\mathbf{x}_{k,m}) \tag{28}$$

where

$${}^M\mathbf{x}_{k,m} = [(\mathbf{x}^{P_{i(1,k,m)}}_{T_{1,k,m}})^{\mathrm{T}}(\mathbf{x}^{P_{i(2,k,m)}}_{T_{2,k,m}})^{\mathrm{T}}, \ldots, (\mathbf{x}^{P_{i(f_m,k,k,m)}}_{T_{M_{k,m},k,m}})^{\mathrm{T}}]^{\mathrm{T}};$$

$$\mathbf{S}^2_{k,j} = [\boldsymbol{\theta}^{\mathrm{T}}_{i(1,k,m)}\boldsymbol{\theta}^{\mathrm{T}}_{i(2,k,m)}, \ldots, \boldsymbol{\theta}^{\mathrm{T}}_{i(M_{k,m},k,j)}]^{\mathrm{T}}, \quad \boldsymbol{\theta}_{i(*,k,j)}$$

$(* = 1, 2, \ldots, M_{k,m})$ is a $6 \times 6S$ matrix consisting of S submatrices with the dimension of 6×6, and the $i(*,k,m)$th submatrix is an identity matrix and others are zero matrices; $\mathbf{C}^1_{k,m} = \mathrm{diag}\{\mathbf{M}^{P_{i(*,k,m)}}_{T_{*,k,m}}\}$; $c_{k,m}$ is an $1 \times 6M_{k,m}$ row vector, representing the linear combination of the $M_{k,m}$ features. It is determined by the measuring plan.

Proof: For a feature, "$*, k, m$", that is involved in calculating the mth KPC at stage k, it is needed to derive the DMV of $T_i, (*,k,m)$ w.r.t. R, i.e., $\mathbf{x}^R_{T_{*,k,m}}$. Given $\mathbf{x}^R_{P_{i(*,k,m)}}$ and $\mathbf{x}^{P_{i(*,k,m)}}_{T_{*,k,m}}$, it can be derived by applying Lemma 1

$$\mathbf{x}^{P_{i(*,k,m)}}_{T_{*,k,m}} = \mathbf{M}^{P_{i(*,k,m)}}_{T_{*,k,m}} \cdot \mathbf{x}^R_{P_{i(*,k,m)}} + \mathbf{x}^{P_{i(*,k,m)}}_{T_{*,k,m}} \tag{29}$$

where $\mathbf{x}^R_{P_{i(*,k,m)}}$ is selected from $\mathbf{x}_k$, i.e., $\mathbf{x}^R_{P_{i(*,k,m)}} = \boldsymbol{\theta}_{i(*,k,j)} \cdot \mathbf{x}_k$. It is straightforward to stack up the components in (29) to form $\mathbf{C}^1_{k,m}$, $\mathbf{S}^2_{k,j}$, and ${}^M\mathbf{x}_{k,m}$ in (28).

The deviations of the mth KPC measured at stage k is modeled by (28), which can be expanded to all M_k KPCs.

Corollary 9.1: The deviations of all M_k KPCs measured at stage k can be derived as

$$\mathbf{y}_k = \mathbf{C}^2_k \cdot \mathbf{C}^1_k \cdot \mathbf{C}^0_k \cdot \mathbf{x}_k + \mathbf{C}^2_k \cdot {}^M\mathbf{u}_k \tag{30}$$

where $\mathbf{C}^2_k = [(\mathbf{c}_{k,1})^{\mathrm{T}}, \ldots, (\mathbf{c}_{k,M_k})^{\mathrm{T}}]^{\mathrm{T}}$, $\mathbf{C}^1_k = \mathrm{diag}\left\{\mathbf{C}^1_{k,m}\right\}$, $\mathbf{C}^0_k = [(\mathbf{S}^2_{k,1})^{\mathrm{T}}(\mathbf{S}^2_{k,2})^{\mathrm{T}}, \ldots, (\mathbf{S}^2_{k,M_k})^{\mathrm{T}}]^{\mathrm{T}}$, and ${}^M\mathbf{u}_k = [({}^M\mathbf{x}_{k,1})^{\mathrm{T}}({}^M\mathbf{x}_{k,2})^{\mathrm{T}}, \ldots, ({}^M\mathbf{x}_{k,M_k})^{\mathrm{T}}]^{\mathrm{T}}$.

It should be noted that the term $\mathbf{C}^2_k \cdot {}^M\mathbf{u}_k$ reflects the KPC deviations induced by the deviations of features on the parts, when they are fabricated. Denoting $\mathbf{u}_k = [({}^S\mathbf{u}_k)^{\mathrm{T}}\ ({}^F\mathbf{u}_k)^{\mathrm{T}}\ ({}^O\mathbf{u}_k)^{\mathrm{T}}\ ({}^M\mathbf{u}_k)^{\mathrm{T}}]^{\mathrm{T}}$ as the combination of all the deviations induced by both assembly operations and part fabrication processes, the system matrices in model (12) are

$$\mathbf{A}_k = \mathbf{I}_{6S\times 6S} + \mathbf{A}^4_k \cdot \mathbf{A}^2_k \cdot \mathbf{A}^1_k \cdot \mathbf{A}^0_k \tag{31}$$

$$\mathbf{B}_k = [\,\mathbf{A}^4_k \cdot \mathbf{A}^2_k \quad \mathbf{A}^4_k \cdot \mathbf{A}^3_k \quad \mathbf{I}_{6S\times 6S} \quad \mathbf{0}_{6S\times 6M_k}\,] \tag{32}$$

$$\mathbf{C}_k = \mathbf{C}^2_k \cdot \mathbf{C}^1_k \cdot \mathbf{C}^0_k \tag{33}$$

and

$$\mathbf{D}_k = [\,\mathbf{0}_{M_k\times(36J_k+6J_k+6S)} \quad \mathbf{C}^2_k\,] \tag{34}$$

where $\mathbf{0}_{c\times d}$ is a $c \times d$ matrix with all zero elements. Equations (31)–(34) define the system matrices of the model in (12).

The input information of the model (12) is obtained from engineering knowledge about the product, process, fixture system, and measurement system. Input vector $\mathbf{u}_k$ is composed of four components, corresponding to four types of process variation sources: ${}^S\mathbf{u}_k$ and ${}^M\mathbf{u}_k$ are deviations of all datum features and measurement features that are generated in the part fabrication processes, respectively. The magnitudes of their variations are provided by the part suppliers. ${}^F\mathbf{u}_k$ represents fixture locator deviations, whose variation magnitudes are provided by the fixture suppliers. The operation variation that represented by ${}^O\mathbf{u}_k$ can be determined by the further study of the variation introduced by part flexibility and other operation conditions. Unmodeled deviations represented in $\mathbf{w}_k$ are introduced to the model by the linearization in deriving (4). Thus, their magnitudes can be determined by estimating the ignored higher order values of

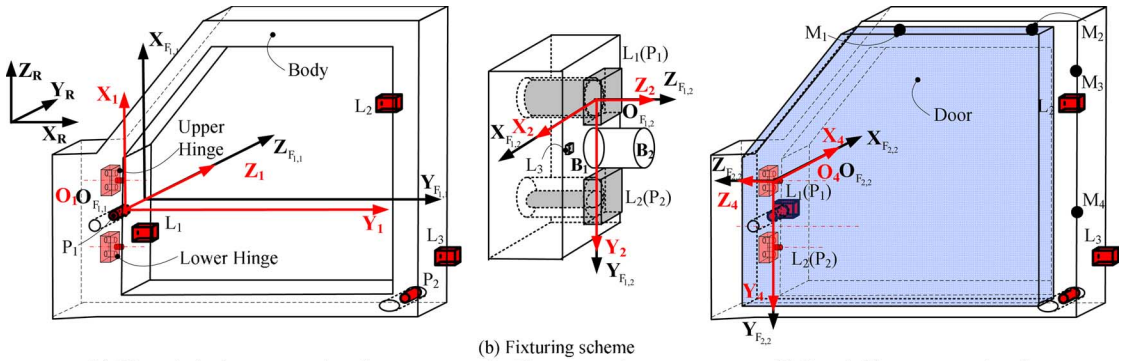

Fig. 5. Illustration of the two-stage door-fitting process.

linearization. Finally, magnitudes of measurement noise $\mathbf{v}_k$ are provided by measurement system specifications or calibrations.

Fully determined by the product and the process design, the final state space model may contain sparse system matrices. The sparse matrices may cause computational problems when the model is used in process diagnosis. This diagnosibility issue has been studied in [24]. However, on the other hand, those zero coefficients in sparse matrices indicate that some variation sources have no impacts on certain sets of KPCs. This indication creates the opportunity to decouple the process accordingly and divide a complex whole process into small subprocesses without losing model accuracy.

IV. Case Study

The variation propagation model of a 3-D rigid-body door-fitting process is derived and applied to the variation analysis for design evaluation.

A. Process Description

A door-fitting process is used to fit a front door to the body of a car by two assembly stages ($N = 2$), as illustrated in Fig. 5. In the first stage, a car body (Part 1, PCS: $\mathrm{O_1X_1Y_1Z_1}$) is located with a pin-hole fixturing scheme. Two hinges [e.g., Part 2, PCS: $\mathrm{O_2X_2Y_2Z_2}$, as shown in Fig. 5(b)], each of which is located by a pin-hole fixturing scheme, are mounted to the body. At the second stage, the subassembly will be located on the same fixture used to locate the car body at the first stage, and the upper hinge (Part 2, PCS: $\mathrm{O_2X_2Y_2Z_2}$) and the lower hinge (Part 3, PCS, is similarly defined as $\mathrm{O_3X_3Y_3Z_3}$) are used as fixture locators for the door (Part 4, PCS: $\mathrm{O_4X_4Y_4Z_4}$). The KPCs are the seal-gap measured at four points $(\mathrm{M_1 - M_4})$. The seal-gap is defined as the distance between the body and the door on those points $(\mathrm{M_1 - M_4})$ along the Y direction in the RCS.

The geometric information of the product and the process is summarized in Table I through Table V. To derive the coefficients in system matrices of the state space model, PCSs for all the four parts $(S = 4)$ are defined and their vectorial representations w.r.t. RCS are listed in Table I. The origin of the RCS is located in the middle of a car's front face. At stage 2, the pins on the upper hinge and the lower hinge will be used as the four-way pin and the two-way pin, respectively. Their coordinates in PCSs are listed in Table II. The KPCs are the distance between the door and the body at the four measurement points. Four measurement features are defined on both $\mathrm{P_1}$ and $\mathrm{P_4}$ and their vectorial representation w.r.t. corresponding PCSs are listed in Table III.

TABLE I
Product Information: Parts

Part	$\mathbf{t}^R_{P_*}$	$\boldsymbol{\omega}^R_{P_*}$
$\mathrm{P_1}$ (body)	[2470.0 836.8 1406.0]^T	[-π/2 −π/2 0]^T
$\mathrm{P_2}$ (Upper Hinge)	[2506.6 865.6 1606.9]^T	[0 π/2 −π/2]^T
$\mathrm{P_3}$ (Lower Hinge)	[2506.6 879.3 1257.5]^T	[0 π/2 −π/2]^T
$\mathrm{P_4}$ (door)	[2506.6 865.6 1564.4]^T	[0 -π/2 π/2]^T

TABLE II
Product Information: Feature Locators

Feature	$\mathbf{t}^{P_*}_{T_*}$	$\boldsymbol{\omega}^{P_*}_{T_*}$
$\mathrm{B_1}$ (on hinge)	[0.0 42.5 0.0]^T	[0 0 0]^T
$\mathrm{B_2}$ (on hinge)	[0.0 42.5 0.0]^T	[0 0 0]^T

TABLE III
Product Information: Measurement Features

Feature	$\mathbf{t}^{P_*}_{T_*}$	$\boldsymbol{\omega}^{P_*}_{T_*}$
$\mathrm{M_1}$ (on body)	[720.5 1005.2 -206.9]^T	[0 π 0]^T
$\mathrm{M_2}$ (on body)	[632.8 1082.9 -161.1]^T	[0 π 0]^T
$\mathrm{M_3}$ (on body)	[-238.4 820.2 -62.8]^T	[0 π 0]^T
$\mathrm{M_4}$ (on body)	[-333.1 570.5 -62.8]^T	[0 π 0]^T
$\mathrm{M_1}$ (on door)	[-235.7 -562.1 -968.6]^T	[0 -π/2 π/2]^T
$\mathrm{M_2}$ (on door)	[-189.9 -474.3 -1046.3]^T	[0 -π/2 π/2]^T
$\mathrm{M_3}$ (on door)	[-91.5 396.9 -783.7]^T	[0 -π/2 π/2]^T
$\mathrm{M_4}$ (on door)	[-91.5 491.6 -533.9]^T	[0 -π/2 π/2]^T

Table IV presents the coordinates of parts w.r.t. the nominal FCSs of corresponding fixtures that locate the parts. The fixture configuration information, represented as the fixture locators' coordinates in FCSs, is summarized in Table V. It is straightforward to define the LCSs of datum features on parts according to the guideline in Fig. 2(b.2). Their coordinates can be derived based on the information in Table V.

B. State Space Model Derivation

A state space model is developed following the procedure introduced in Section III and the nominal product/process design information summarized above. The state vector is composed of four DMVs, corresponding to these four parts.

TABLE IV
PROCESS INFORMATION: FIXTURES-PART RELATION

Fixture	Part	$\mathbf{t}_{P_\bullet}^{F_\bullet}$	$\boldsymbol{\omega}_{P_\bullet}^{F_\bullet}$
$F_{1,1}$	P_1	$[0.0 \quad 0.0 \quad -60.5]^T$	$[0 \quad 0 \quad 0]^T$
$F_{1,2}$	P_2	$[0.0 \quad 0.0 \quad 0.0]^T$	$[0 \quad 0 \quad 0]^T$
$F_{1,3}$	P_3	$[0.0 \quad 0.0 \quad 0.0]^T$	$[0 \quad 0 \quad 0]^T$
$F_{2,1}$	P_1	$[0.0 \quad 0.0 \quad -60.5]^T$	$[0 \quad 0 \quad 0]^T$
	P_2	$[200.9 \quad 36.6 \quad 89.3]^T$	$[\pi/2 \quad \pi/2 \quad 0]^T$
	P_3	$[-148.5 \quad 50.3 \quad 103.1]^T$	$[\pi/2 \quad \pi/2 \quad 0]^T$
$F_{2,2}$	P_4	$[0.0 \quad 0.0 \quad 0.0]^T$	$[0 \quad 0 \quad 0]^T$

TABLE V
PROCESS INFORMATION: FIXTURE LOCATORS

Fixture	$(L_{hx}^{{}^0F_{k,j}}, L_{hy}^{{}^0F_{k,j}}, L_{hz}^{{}^0F_{k,j}})$		$(P_{wx}^{{}^0F_{k,j}}, P_{wy}^{{}^0F_{k,j}}, P_{wz}^{{}^0F_{k,j}})$	
$F_{1,1}$ ($F_{2,1}$)	L_1	$[-325.9 \quad 198.0 \quad 0.0]^T$	P_1	$[0.0 \quad 0.0 \quad -60.5]^T$
	L_2	$[694.9 \quad 988.2 \quad -111.9]^T$	P_2	$[-429.0 \quad 1296.0 \quad -41.6]^T$
	L_3	$[-261.7 \quad 1131.2 \quad 2.26]^T$	P_3	$[0.0 \quad 0.0 \quad -60.5]^T$
$F_{1,2}$ ($F_{1,3}$)	L_1	$[0.0 \quad 0.0 \quad 0.0]^T$	P_1	$[0.0 \quad 0.0 \quad 0.0]^T$
	L_2	$[0.0 \quad 85.0 \quad 0.0]^T$	P_2	$[0.0 \quad 85.0 \quad 0.0]^T$
	L_3	$[20.0 \quad 42.5 \quad 0.0]^T$	P_3	$[0.0 \quad 0.0 \quad 0.0]^T$
$F_{2,2}$	L_1	$[0.0 \quad 0.0 \quad 0.0]^T$	P_1	$[0.0 \quad 0.0 \quad 0.0]^T$
	L_2	$[0.0 \quad 350.0 \quad 0.0]^T$	P_2	$[0.0 \quad 350.0 \quad 0.0]^T$
	L_3	$[-30.0 \quad 175.0 \quad 0.0]^T$	P_3	$[0.0 \quad 0.0 \quad 0.0]^T$

At each stage, based on the fixturing scheme design, selector matrix $\mathbf{S}_{k,j}^1$ are set to assign datum features. At step S1, coordinates of these datum features' in PCSs are used to derive a set of $\mathbf{M}_{T_\bullet,k,j}^{P_{i(\bullet,k,j)}}$, as defined in Lemma 4, to describe the impacts of datum feature deviations. This information is further used at step S2 to model the reorientation derivation. The coordinates of datum features and locating points in FCSs are used in deriving $\mathbf{T}_{1,k,j}$, $\mathbf{T}_{2,k,j}$, $\mathbf{T}_{3,k,j}$, $\mathbf{T}_{4,k,j}^*$, $\mathbf{T}_{5,k,j}^*$, and $\mathbf{T}_{6,k,j}^*$, as defined in Lemma 5. At step S3, the fixture configuration information, as summarized in Table V, is used to derive the coefficients in matrices $\mathbf{T}_{k,j}$, as defined in Lemma 6. Thus, the fixture induced deviation can be described. At stage 2, the upper hinge and the lower hinge will be used as two matting features to locate P_4. In order to model their deviations as that of the fixture locator pins', information in Table II is used to derive $\mathbf{G}_{k,j}$, and their diagonal block matrices $\mathbf{M}_{T_\circ,k,j}^{P_{i(\circ,k,j)}}$, as defined in Lemma 2. Finally, at step S5, the coordinates in Table IV are used to calculate $\mathbf{M}_{P_{r(c,k,j)}}^{{}^0F_{k,j}}$ and model the overall deviations induced at stage k, as defined in Lemma 8.

Since there is no measurement collected after the first stage, $\mathbf{C}_1$ is not considered. To derive the observation matrix $\mathbf{C}_2$, measurement feature coordinates in Table III and the PCSs coordinates in Table I will be used to calculate $\mathbf{C}_{k,m}^1$ and $\mathbf{M}_{T_*,k,m}^{P_{i(*,k,m)}}$, as defined in Lemma 9.

C. Variation Analysis

The variation propagation model can be used in variation analysis to evaluate the product quality of a MAP. The system matrices of the state space model derived in previous section are used to analytically derive the variance of KPCs, i.e., the seal-gap measured at $\mathbf{M}_1 \sim \mathbf{M}_4$. Based on the state space model in the form of (12), the input/out model can be derived to directly link the process variables $\mathbf{u}_k$'s and the quality variables $\mathbf{y}_N$. Variation analysis can be performed by plugging the variance of $\mathbf{u}_k$'s and calculating that of $\mathbf{y}_N$. Since no simulation is needed, the time for analysis depends only on the computational speed of computers.

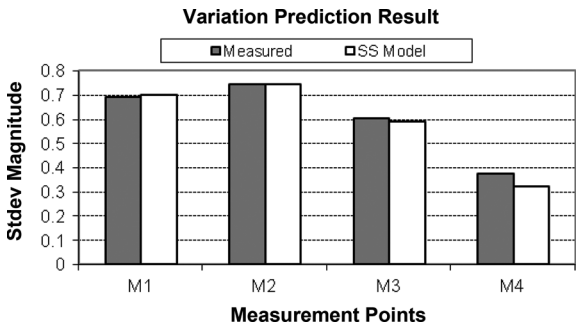

Fig. 6. Variation analysis result comparison.

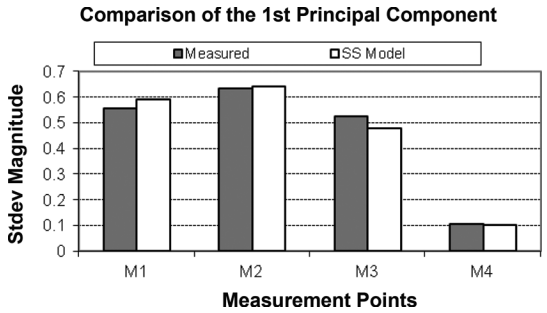

Fig. 7. Variation pattern comparison.

The variation analysis is conducted under the normal condition, i.e., there is no excessive faulty variation introduced into the MAP by variation sources. The magnitudes of the variances of the variation sources are determined according to the nominal fixture tolerances and part tolerances, whereas the magnitudes of measurement noises are determined by specifications of measurement devices. Since the magnitudes of random variations are assumed small and the dimensions of parts are relatively large, the unmodeled noises caused by the second order small values in linearization are neglected.

The standard deviations of KPCs are then calculated based on the developed state space model. These analytic values are compared with measurement data of 25 cars collected from real-production under a normal production condition. As shown in Fig. 6, the discrepancies between the model-based analytic variances and that calculated from the real measurements are reasonably small. This small discrepancies show that the model captures the dominant impacts of variation sources correctly. The variance/covariance structure of multivariate KPCs is also checked by conducting principal component analysis. The eigenvector corresponding to the largest eigenvalue of the covariance matrices of the measured data are selected. It account for more than 90% of total variance. As shown in Fig. 7, the dominant covariance structure of KPCs is also correctly captured.

V. CONCLUSION

Complex correlations among different stages of a MAP make it difficult for engineers to understand the product quality variation propagation along stages. It significantly impede the al-

ternative product/process design evaluation and process variation source identification. In this paper, an variation propagation modeling technique is proposed based on the DMV representation. The model is presented in a state space model format, for which a systematic procedure has been developed. Compared with the existing MAP modeling techniques, the proposed one is more generic by covering both Type-I and Type-II assembly and by considering the impacts of deviations induced by part fabrication processes. The proposed modeling technique is validated by comparing the state-space-model-based analytic variance with that calculated from real-production data in a door fitting process.

The proposed 3-D state space model for MAPs has great potentials for various applications to achieve quality assurance in a MAP: 1) Since the interactions between process variables (i.e., fixture locators deviations) and quality variables (i.e., KPC deviations) are mathematically represented, variation source identification can be conducted by collecting KPC measurement data and solving the equations. 2) This model can also be used as a tool for quality assured product or process design. By providing an explicit model that links model coefficient with design parameters, product/process design can be optimized and will be able to cost-effectively deliver good quality. This strategy moves the quality assurance to the early stage of production realization and will reinforce total quality management. 3) The structure of the proposed state space model makes it possible to adopt some of the well developed control theories to solve engineering problems related to quality engineering, e.g., diagnosability study and sensor placement. 4) Since the deviations of features that caused by part fabrication process are explicitly modeled, the variation sources can be traced back to upstream production stages so that product designer can either use the model to assign tolerances to different part suppliers, or conduct tolerance synthesis among different parts to improve quality and reduce manufacturing costs.

APPENDIX I

For the general 3-2-1 fixture locating scheme, as shown in Fig. 2(a), the coefficient matrix $\mathbf{T}_{k,j}$ is defined as shown in (A1) at the bottom of the page, where

$$\begin{aligned} C_{11} = {} & L_{3x}^{{}^0F_{k,j}} L_{1y}^{{}^0F_{k,j}} - L_{1y}^{{}^0F_{k,j}} L_{2x}^{{}^0F_{k,j}} + L_{3y}^{{}^0F_{k,j}} L_{2x}^{{}^0F_{k,j}} \\ & + L_{2y}^{{}^0F_{k,j}} L_{1x}^{{}^0F_{k,j}} - L_{2y}^{{}^0F_{k,j}} L_{3x}^{{}^0F_{k,j}} \\ & - L_{3y}^{{}^0F_{k,j}} L_{1x}^{{}^0F_{k,j}}. \end{aligned} \tag{A2}$$

For the pin-hole fixturing scheme shown in Fig. 2(b), fixture locator deviation can be alternatively represented as $\mathbf{u}_{k,j}^{{}^0F_{k,j}} = \left[\Delta L_{1z}^{{}^0F_{k,j}} \Delta L_{2z}^{{}^0F_{k,j}} \Delta L_{3z}^{{}^0F_{k,j}} \;\; \Delta P_{1x}^{{}^0F_{k,j}} \Delta P_{2x}^{{}^0F_{k,j}} \Delta P_{3y}^{{}^0F_{k,j}}\right]^{\mathrm{T}}$, and the coefficient matrix is defined as shown in (A3) at the bottom of the next page.

APPENDIX II

Given the six datum features defined in Section II, matrices $\mathbf{T}_{1,k,j}$ through $\mathbf{T}_{6,k,j}$ can be derived by investigating the six

$$\mathbf{T}_{k,j} = \begin{bmatrix} \frac{\left(L_{2y}^{{}^0F_{k,j}} - L_{3y}^{{}^0F_{k,j}}\right) P_{1z}^{{}^0F_{k,j}}}{C_{11}} & \frac{\left(L_{3y}^{{}^0F_{k,j}} - L_{1y}^{{}^0F_{k,j}}\right) P_{1z}^{{}^0F_{k,j}}}{C_{11}} & \frac{P_{1y}^{{}^0F_{k,j}}}{\left(P_{1y}^{{}^0F_{k,j}} - P_{2y}^{{}^0F_{k,j}}\right)} & 0 \\ \frac{\left(L_{3x}^{{}^0F_{k,j}} - L_{2x}^{{}^0F_{k,j}}\right) P_{3z}^{{}^0F_{k,j}}}{C_{11}} & \frac{\left(L_{1x}^{{}^0F_{k,j}} - L_{3x}^{{}^0F_{k,j}}\right) P_{3z}^{{}^0F_{k,j}}}{C_{11}} & \frac{-P_{3x}^{{}^0F_{k,j}}}{\left(P_{1y}^{{}^0F_{k,j}} - P_{2y}^{{}^0F_{k,j}}\right)} & 1 \\ \frac{L_{3y}^{{}^0F_{k,j}} L_{2x}^{{}^0F_{k,j}} - L_{2y}^{{}^0F_{k,j}} L_{3x}^{{}^0F_{k,j}}}{C_{11}} & \frac{L_{3x}^{{}^0F_{k,j}} L_{1y}^{{}^0F_{k,j}} - L_{3y}^{{}^0F_{k,j}} L_{1x}^{{}^0F_{k,j}}}{C_{11}} & 0 & 0 \\ \frac{L_{2x}^{{}^0F_{k,j}} - L_{3x}^{{}^0F_{k,j}}}{C_{11}} & \frac{L_{3x}^{{}^0F_{k,j}} - L_{1x}^{{}^0F_{k,j}}}{C_{11}} & 0 & 0 \\ \frac{L_{2y}^{{}^0F_{k,j}} - L_{3y}^{{}^0F_{k,j}}}{C_{11}} & \frac{L_{3y}^{{}^0F_{k,j}} - L_{1y}^{{}^0F_{k,j}}}{C_{11}} & 0 & 0 \\ 0 & 0 & \frac{1}{\left(P_{1y}^{{}^0F_{k,j}} - P_{2y}^{{}^0F_{k,j}}\right)} & \frac{-1}{\left(P_{1y}^{{}^0F_{k,j}} - P_{2y}^{{}^0F_{k,j}}\right)} \end{bmatrix} \begin{matrix} 0 \\ 0 \\ 0 \\ 0 \\ 0 \\ 0 \\ 0 \end{matrix} \tag{A1}$$

datum points where fixture locating pins and datum features touch each other. It is assumed that datum points q_1, q_2, and q_3 are the datum points in touch with the three primary datum features $p_{1,k,j}$, $p_{2,k,j}$, and $p_{3,k,j}$, respectively; q_4 and q_5 touch with the secondary datum features, $s_{1,k,j}$ and $s_{2,k,j}$, respectively, and q_6 touch with the tertiary datum feature $\mathbf{t}_{k,j}$. The nominal coordinates of these six points in $F_{k,j}$ are denoted as $\mathbf{q}_1^{F_{k,j}}$, $\mathbf{q}_2^{F_{k,j}}$, $\mathbf{q}_3^{F_{k,j}}$, $\mathbf{q}_4^{F_{k,j}}$, $\mathbf{q}_5^{F_{k,j}}$ and $\mathbf{q}_6^{F_{k,j}}$, respectively. Denoting $\tilde{\mathbf{q}} = [\mathbf{q}^{\mathrm{T}} \quad 1]^{\mathrm{T}}$, the coordinates of point q_1 w.r.t. datum feature $\tilde{\mathbf{q}}_1^{p_{1,k,j}}$ can be achieved by performing homogeneous transformation twice, i.e., from $F_{k,j}$ to RCS and from RCS to LCS of $p_{1,k,j}$. With the same strategy, following transformation relationships can be obtained:

$$\begin{cases} \mathbf{H}_R^{p_{1,k,j}} \mathbf{H}_{F_{k,j}}^R \tilde{\mathbf{q}}_1^{F_{k,j}} = \tilde{\mathbf{q}}_1^{p_{1,k,j}} \\ \mathbf{H}_R^{p_{2,k,j}} \mathbf{H}_{F_{k,j}}^R \tilde{\mathbf{q}}_2^{F_{k,j}} = \tilde{\mathbf{q}}_2^{p_{2,k,j}} \\ \mathbf{H}_R^{p_{3,k,j}} \mathbf{H}_{F_{k,j}}^R \tilde{\mathbf{q}}_3^{F_{k,j}} = \tilde{\mathbf{q}}_3^{p_{3,k,j}} \\ \mathbf{H}_R^{s_{1,k,j}} \mathbf{H}_{F_{k,j}}^R \tilde{\mathbf{q}}_4^{F_{k,j}} = \tilde{\mathbf{q}}_4^{s_{1,k,j}} \\ \mathbf{H}_R^{s_{2,k,j}} \mathbf{H}_{F_{k,j}}^R \tilde{\mathbf{q}}_5^{F_{k,j}} = \tilde{\mathbf{q}}_5^{s_{2,k,j}} \\ \mathbf{H}_R^{t_{k,j}} \mathbf{H}_{F_{k,j}}^R \tilde{\mathbf{q}}_6^{F_{k,j}} = \tilde{\mathbf{q}}_6^{t_{k,j}} \end{cases}. \tag{A4}$$

$$\mathbf{T}_{k,j} = \begin{bmatrix} 0 & 0 \\ 0 & 0 \\ \dfrac{\left(L_{3y}^{\,0F_{k,j}} L_{2x}^{\,0F_{k,j}} - L_{2y}^{\,0F_{k,j}} L_{3x}^{\,0F_{k,j}}\right)}{C_{11}} & \dfrac{\left(L_{3x}^{\,0F_{k,j}} L_{1y}^{\,0F_{k,j}} - L_{3y}^{\,0F_{k,j}} L_{1x}^{\,0F_{k,j}}\right)}{C_{11}} \\ \dfrac{\left(L_{2x}^{\,0F_{k,j}} - L_{3x}^{\,0F_{k,j}}\right)}{C_{11}} & \dfrac{\left(L_{3x}^{\,0F_{k,j}} - L_{1x}^{\,0F_{k,j}}\right)}{C_{11}} \\ \dfrac{\left(L_{2y}^{\,0F_{k,j}} - L_{3y}^{\,0F_{k,j}}\right)}{C_{11}} & \dfrac{\left(L_{3y}^{\,0F_{k,j}} - L_{1y}^{\,0F_{k,j}}\right)}{C_{11}} \\ 0 & 0 \end{bmatrix}$$
$$\begin{bmatrix} 0 & 1 & 0 & 0 \\ 0 & 0 & 0 & 1 \\ \dfrac{\left(L_{2y}^{\,0F_{k,j}} L_{1x}^{\,0F_{k,j}} - L_{1y}^{\,0F_{k,j}} L_{2x}^{\,0F_{k,j}}\right)}{C_{11}} & 0 & 0 & 0 \\ \dfrac{\left(L_{1x}^{\,0F_{k,j}} - L_{2x}^{\,0F_{k,j}}\right)}{C_{11}} & 0 & 0 & 0 \\ \dfrac{\left(L_{1y}^{\,0F_{k,j}} - L_{2y}^{\,0F_{k,j}}\right)}{C_{11}} & 0 & 0 & 0 \\ 0 & \dfrac{-1}{P_{2y}^{\,0F_{k,j}}} & \dfrac{1}{P_{2y}^{\,0F_{k,j}}} & 0 \end{bmatrix} \tag{A3}$$

$$\begin{bmatrix} [{}^0\mathbf{a}_{p_{1,k,j}}^{F_{k,j}}]^{\mathrm{T}} [\mathbf{q}_1^{F_{k,j}} \times {}^0\mathbf{a}_{p_{1,k,j}}^{F_{k,j}}]^{\mathrm{T}} \\ [{}^0\mathbf{a}_{p_{2,k,j}}^{F_{k,j}}]^{\mathrm{T}} [\mathbf{q}_2^{F_{k,j}} \times {}^0\mathbf{a}_{p_{2,k,j}}^{F_{k,j}}]^{\mathrm{T}} \\ [{}^0\mathbf{a}_{p_{3,k,j}}^{F_{k,j}}]^{\mathrm{T}} [\mathbf{q}_3^{F_{k,j}} \times {}^0\mathbf{a}_{p_{3,k,j}}^{F_{k,j}}]^{\mathrm{T}} \\ [{}^0\mathbf{a}_{s_{1,k,j}}^{F_{k,j}}]^{\mathrm{T}} [\mathbf{q}_4^{F_{k,j}} \times {}^0\mathbf{a}_{s_{1,k,j}}^{F_{k,j}}]^{\mathrm{T}} \\ [{}^0\mathbf{a}_{s_{2,k,j}}^{F_{k,j}}]^{\mathrm{T}} [\mathbf{q}_5^{F_{k,j}} \times {}^0\mathbf{a}_{s_{2,k,j}}^{F_{k,j}}]^{\mathrm{T}} \\ [{}^0\mathbf{a}_{t_{k,j}}^{F_{k,j}}]^{\mathrm{T}} [\mathbf{q}_6^{F_{k,j}} \times {}^0\mathbf{a}_{t_{k,j}}^{F_{k,j}}]^{\mathrm{T}} \end{bmatrix} \cdot \mathbf{x}_{F_{k,j}}^R$$
$$= \begin{bmatrix} \left[\boldsymbol{\theta}_{p_{1,k,j}}^R \times {}^0\mathbf{n}_{F_{k,j}}^{p_{1,k,j}}\right]_{(3)} \left[\boldsymbol{\theta}_{p_{1,k,j}}^R \times {}^0\mathbf{o}_{F_{k,j}}^{p_{1,k,j}}\right]_{(3)} \left[\boldsymbol{\theta}_{p_{1,k,j}}^R \times {}^0\mathbf{a}_{F_{k,j}}^{p_{1,k,j}}\right]_{(3)} \left[\boldsymbol{\theta}_{p_{1,k,j}}^R \times {}^0\mathbf{t}_{F_{k,j}}^{p_{1,k,j}} + \mathbf{d}_{p_{1,k,j}}^R\right]_{(3)} \end{bmatrix} \cdot \tilde{\mathbf{q}}_1^{F_{k,j}} \\ \begin{bmatrix} \left[\boldsymbol{\theta}_{p_{2,k,j}}^R \times {}^0\mathbf{n}_{F_{k,j}}^{p_{2,k,j}}\right]_{(3)} \left[\boldsymbol{\theta}_{p_{2,k,j}}^R \times {}^0\mathbf{o}_{F_{k,j}}^{p_{2,k,j}}\right]_{(3)} \left[\boldsymbol{\theta}_{p_{2,k,j}}^R \times {}^0\mathbf{a}_{F_{k,j}}^{p_{2,k,j}}\right]_{(3)} \left[\boldsymbol{\theta}_{p_{2,k,j}}^R \times {}^0\mathbf{t}_{F_{k,j}}^{p_{2,k,j}} + \mathbf{d}_{p_{2,k,j}}^R\right]_{(3)} \end{bmatrix} \cdot \tilde{\mathbf{q}}_2^{F_{k,j}} \\ \begin{bmatrix} \left[\boldsymbol{\theta}_{p_{3,k,j}}^R \times {}^0\mathbf{n}_{F_{k,j}}^{p_{3,k,j}}\right]_{(3)} \left[\boldsymbol{\theta}_{p_{3,k,j}}^R \times {}^0\mathbf{o}_{F_{k,j}}^{p_{3,k,j}}\right]_{(3)} \left[\boldsymbol{\theta}_{p_{3,k,j}}^R \times {}^0\mathbf{a}_{F_{k,j}}^{p_{3,k,j}}\right]_{(3)} \left[\boldsymbol{\theta}_{p_{3,k,j}}^R \times {}^0\mathbf{t}_{F_{k,j}}^{p_{3,k,j}} + \mathbf{d}_{p_{3,k,j}}^R\right]_{(3)} \end{bmatrix} \cdot \tilde{\mathbf{q}}_3^{F_{k,j}} \\ \begin{bmatrix} \left[\boldsymbol{\theta}_{s_{1,k,j}}^R \times {}^0\mathbf{n}_{F_{k,j}}^{s_{1,k,j}}\right]_{(3)} \left[\boldsymbol{\theta}_{s_{1,k,j}}^R \times {}^0\mathbf{o}_{F_{k,j}}^{s_{1,k,j}}\right]_{(3)} \left[\boldsymbol{\theta}_{s_{1,k,j}}^R \times {}^0\mathbf{a}_{F_{k,j}}^{s_{1,k,j}}\right]_{(3)} \left[\boldsymbol{\theta}_{s_{1,k,j}}^R \times {}^0\mathbf{t}_{F_{k,j}}^{s_{1,k,j}} + \mathbf{d}_{s_{1,k,j}}^R\right]_{(3)} \end{bmatrix} \cdot \tilde{\mathbf{q}}_4^{F_{k,j}} \\ \begin{bmatrix} \left[\boldsymbol{\theta}_{s_{2,k,j}}^R \times {}^0\mathbf{n}_{F_{k,j}}^{s_{2,k,j}}\right]_{(3)} \left[\boldsymbol{\theta}_{s_{2,k,j}}^R \times {}^0\mathbf{o}_{F_{k,j}}^{s_{2,k,j}}\right]_{(3)} \left[\boldsymbol{\theta}_{s_{2,k,j}}^R \times {}^0\mathbf{a}_{F_{k,j}}^{s_{2,k,j}}\right]_{(3)} \left[\boldsymbol{\theta}_{s_{2,k,j}}^R \times {}^0\mathbf{t}_{F_{k,j}}^{s_{2,k,j}} + \mathbf{d}_{s_{2,k,j}}^R\right]_{(3)} \end{bmatrix} \cdot \tilde{\mathbf{q}}_5^{F_{k,j}} \\ \begin{bmatrix} \left[\boldsymbol{\theta}_{t_{k,j}}^R \times {}^0\mathbf{n}_{F_{k,j}}^{t_{k,j}}\right]_{(3)} \left[\boldsymbol{\theta}_{t_{k,j}}^R \times {}^0\mathbf{o}_{F_{k,j}}^{t_{k,j}}\right]_{(3)} \left[\boldsymbol{\theta}_{t_{k,j}}^R \times {}^0\mathbf{a}_{F_{k,j}}^{t_{k,j}}\right]_{(3)} \left[\boldsymbol{\theta}_{t_{k,j}}^R \times {}^0\mathbf{t}_{F_{k,j}}^{t_{k,j}} + \mathbf{d}_{t_{k,j}}^R\right]_{(3)} \end{bmatrix} \cdot \tilde{\mathbf{q}}_6^{F_{k,j}} \end{bmatrix} \tag{A8}$$

When the parts are located, six locating pins are in touch with the six datum features. Therefore, points q_1 though q_6 will be right on the datum feature. Since the z direction is defined as the normal direction of the surface, the z coordinates of these six points, w.r.t corresponding datum feature, will be zeros, i.e., $\left[\tilde{\mathbf{q}}_i^{\bullet,k,j}\right]_{(3)} = 0$ for $i = 1, 2, \ldots, 6$ and $\bullet \in \{p_1, p_2, p_3, s_1, s_2, t\} \cdot [\mathrm{v}]_{(3)}$ denotes the third (3rd) element of vector v. [8] shows that q_1 touching $p_{1,k,j}$ leads to

$$\left[\boldsymbol{\Delta}^R_{p_{1,k,j}} \cdot {}^0\mathbf{H}^{p_{1,k,j}}_{F_{k,j}} \cdot \tilde{\mathbf{q}}_1^{F_{k,j}}\right]_{(3)} = \left[\boldsymbol{\Delta}^R_{p_{1,k,j}} \cdot {}^0\mathbf{H}^{p_{1,k,j}}_{F_{k,j}} \cdot \tilde{\boldsymbol{q}}_1^{F_{k,j}}\right]_{(3)} \tag{A5}$$

where

$$\boldsymbol{\Delta}^R_{p_{1,k,j}} = \begin{bmatrix} \hat{\boldsymbol{\theta}}^R_{p_{1,k,j}} & \mathbf{d}^R_{p_{1,k,j}} \\ \mathbf{0} & 0 \end{bmatrix}$$

and

$${}^0\mathbf{H}^{p_{1,k,j}}_{F_{k,j}} = \begin{bmatrix} {}^0\mathbf{n}^{p_{1,k,j}}_{F_{k,j}} & {}^0\mathbf{o}^{p_{1,k,j}}_{F_{k,j}} & {}^0\mathbf{a}^{p_{1,k,j}}_{F_{k,j}} & {}^0\mathbf{t}^{p_{1,k,j}}_{F_{k,j}} \\ 0 & 0 & 0 & 1 \end{bmatrix}.$$

(A5) can be further manipulated as

$$\left[\boldsymbol{\Delta}^R_{p_{1,k,j}} {}^0\mathbf{H}^{p_{1,k,j}}_{F_{k,j}} \tilde{\mathbf{q}}_1^{F_{k,j}}\right]_{(3)} = \left[\left[{}^0\mathbf{a}^{F_{k,j}}_{p_{1,k,j}}\right]^{\mathrm{T}} \left[\mathbf{q}_1^{F_{k,j}} \times {}^0\mathbf{a}^{F_{k,j}}_{p_{1,k,j}}\right]^{\mathrm{T}}\right] \mathbf{x}^R_{F_{k,j}} \tag{A6}$$

and

$$\begin{aligned} &\left[\boldsymbol{\Delta}^R_{p_{1,k,j}} \cdot {}^0\mathbf{H}^{p_{1,k,j}}_{F_{k,j}} \cdot \tilde{\mathbf{q}}_1^{F_{k,j}}\right]_{(3)} \\ &\quad = \left[\left[\boldsymbol{\theta}^R_{p_{1,k,j}} \times {}^0\mathbf{n}^{p_{1,k,j}}_{F_{k,j}}\right]_{(3)} \quad \left[\boldsymbol{\theta}^R_{p_{1,k,j}} \times {}^0\mathbf{o}^{p_{1,k,j}}_{F_{k,j}}\right]_{(3)} \right. \\ &\qquad \left[\boldsymbol{\theta}^R_{p_{1,k,j}} \times {}^0\mathbf{a}^{p_{1,k,j}}_{F_{k,j}}\right]_{(3)} \\ &\qquad \left.\left[\boldsymbol{\theta}^R_{p_{1,k,j}} \times {}^0\mathbf{t}^{p_{1,k,j}}_{F_{k,j}} + \mathbf{d}^R_{p_{1,k,j}}\right]_{(3)}\right] \cdot \tilde{\mathbf{q}}_1^{F_{k,j}}. \end{aligned} \tag{A7}$$

The same strategy can be used to derive the other five equations for q_2 though q_6, and the six equations can be combined together to form an equation system as defined in (A8), as shown at the bottom of the previous page.

$$\mathbf{T}_{1,k,j} = \begin{bmatrix} 0 & 0 & 0 & 0 & 0 & 0 \\ 0 & 0 & 0 & 0 & 0 & 0 \\ 0 & 0 & \frac{C_2}{C_1} & \frac{C_2\left(q_{1y}^{F_{k,j}} + {}^0t_{Fy_{k,j}}^{p_{1,k,j}}\right)}{C_1} & -\frac{C_2\left(q_{1x}^{F_{k,j}} + {}^0t_{Fx_{k,j}}^{p_{1,k,j}}\right)}{C_1} & 0 \\ 0 & 0 & \frac{C_3}{C_1} & \frac{C_3\left(q_{1y}^{F_{k,j}} + {}^0t_{Fy_{k,j}}^{p_{1,k,j}}\right)}{C_1} & -\frac{C_3\left(q_{1x}^{F_{k,j}} + {}^0t_{Fx_{k,j}}^{p_{1,k,j}}\right)}{C_1} & 0 \\ 0 & 0 & \frac{C_4}{C_1} & \frac{C_4\left(q_{1y}^{F_{k,j}} + {}^0t_{Fy_{k,j}}^{p_{1,k,j}}\right)}{C_1} & -\frac{C_4\left(q_{1x}^{F_{k,j}} + {}^0t_{Fx_{k,j}}^{p_{1,k,j}}\right)}{C_1} & 0 \\ 0 & 0 & 0 & 0 & 0 & 0 \end{bmatrix}$$

$$\mathbf{T}_{2,k,j} = \begin{bmatrix} 0 & 0 & 0 & 0 & 0 & 0 \\ 0 & 0 & 0 & 0 & 0 & 0 \\ 0 & 0 & -\frac{C_5}{C_1} & -\frac{C_5\left(q_{2y}^{F_{k,j}} + {}^0t_{Fy_{k,j}}^{p_{2,k,j}}\right)}{C_1} & \frac{C_5\left(q_{2x}^{F_{k,j}} + {}^0t_{Fx_{k,j}}^{p_{2,k,j}}\right)}{C_1} & 0 \\ 0 & 0 & -\frac{C_6}{C_1} & -\frac{C_6\left(q_{2y}^{F_{k,j}} + {}^0t_{Fy_{k,j}}^{p_{2,k,j}}\right)}{C_1} & \frac{C_6\left(q_{2x}^{F_{k,j}} + {}^0t_{Fx_{k,j}}^{p_{2,k,j}}\right)}{C_1} & 0 \\ 0 & 0 & -\frac{C_7}{C_1} & -\frac{C_7\left(q_{2y}^{F_{k,j}} + {}^0t_{Fy_{k,j}}^{p_{2,k,j}}\right)}{C_1} & \frac{C_7\left(q_{2x}^{F_{k,j}} + {}^0t_{Fx_{k,j}}^{p_{2,k,j}}\right)}{C_1} & 0 \\ 0 & 0 & 0 & 0 & 0 & 0 \end{bmatrix}$$

and

$$\mathbf{T}_{3,k,j} = \begin{bmatrix} 0 & 0 & 0 & 0 & 0 & 0 \\ 0 & 0 & 0 & 0 & 0 & 0 \\ 0 & 0 & \frac{C_8}{C_1} & \frac{C_8\left(q_{3y}^{F_{k,j}} + {}^0t_{Fy_{k,j}}^{p_{3,k,j}}\right)}{C_1} & \frac{-C_8\left(q_{3x}^{F_{k,j}} + {}^0t_{Fx_{k,j}}^{p_{3,k,j}}\right)}{C_1} & 0 \\ 0 & 0 & \frac{C_9}{C_1} & \frac{C_9\left(q_{3y}^{F_{k,j}} + {}^0t_{Fy_{k,j}}^{p_{3,k,j}}\right)}{C_1} & \frac{-C_9\left(q_{3x}^{F_{k,j}} + {}^0t_{Fx_{k,j}}^{p_{3,k,j}}\right)}{C_1} & 0 \\ 0 & 0 & \frac{C_{10}}{C_1} & \frac{C_{10}\left(q_{3y}^{F_{k,j}} + {}^0t_{Fy_{k,j}}^{p_{3,k,j}}\right)}{C_1} & \frac{-C_{10}\left(q_{3x}^{F_{k,j}} + {}^0t_{Fx_{k,j}}^{p_{3,k,j}}\right)}{C_1} & 0 \\ 0 & 0 & 0 & 0 & 0 & 0 \end{bmatrix}$$

By solving the equation system, we can express the DMV $\mathbf{x}^R_{F_{k,j}}$ as a linear combination of the deviations of datum features, as defined in (11). The fixture locating scheme ensures that all the six degree-of-freedom of the part/subassembly will be constrained. At the mean time, it also guarantees that the inverse of the matrix on the left hand side of (A8) exists [8]. In practice, the primary, secondary and tertiary datum surfaces are often defined to be orthogonal to each other. This standardization, as illustrated in Fig. 2, simplifies the derivation of $\mathbf{T}_{1,k,j}$ through $\mathbf{T}_{6,k,j}$. Given the nominal coordinates of q_1 through q_6 in $F_{k,j}$,

$$\begin{aligned}
\mathbf{q}_1^{F_{k,j}} &= \begin{bmatrix} q_{1x}^{F_{k,j}} & q_{1y}^{F_{k,j}} & 0 \end{bmatrix}^{\mathrm{T}} \\
\mathbf{q}_2^{F_{k,j}} &= \begin{bmatrix} q_{2x}^{F_{k,j}} & q_{2y}^{F_{k,j}} & 0 \end{bmatrix}^{\mathrm{T}} \\
\mathbf{q}_3^{F_{k,j}} &= \begin{bmatrix} q_{3x}^{F_{k,j}} & q_{3y}^{F_{k,j}} & 0 \end{bmatrix}^{\mathrm{T}} \\
\mathbf{q}_4^{F_{k,j}} &= \begin{bmatrix} 0 & q_{4y}^{F_{k,j}} & q_{4z}^{F_{k,j}} \end{bmatrix}^{\mathrm{T}} \\
\mathbf{q}_5^{F_{k,j}} &= \begin{bmatrix} q_{5x}^{F_{k,j}} & q_{5y}^{F_{k,j}} & q_{5z}^{F_{k,j}} \end{bmatrix}^{\mathrm{T}} \\
\mathbf{q}_6^{F_{k,j}} &= \begin{bmatrix} q_{6x}^{F_{k,j}} & 0 & q_{6z}^{F_{k,j}} \end{bmatrix}^{\mathrm{T}}
\end{aligned}$$

and nominal HTM for $F_{k,j}$ w.r.t. the LCSs of three PD features ($p_{1,k,j}$, $p_{2,k,j}$, and $p_{3,k,j}$)

$${}^0\mathbf{H}_{F_{k,j}}^{p_{1,k,j}} = \begin{bmatrix} 1 & 0 & 0 & {}^0t_{Fx_{k,j}}^{p_{1,k,j}} \\ 0 & 1 & 0 & {}^0t_{Fy_{k,j}}^{p_{1,k,j}} \\ 0 & 0 & 1 & 0 \\ 0 & 0 & 0 & 1 \end{bmatrix}$$

$${}^0\mathbf{H}_{F_{k,j}}^{p_{2,k,j}} = \begin{bmatrix} 1 & 0 & 0 & {}^0t_{Fx_{k,j}}^{p_{2,k,j}} \\ 0 & 1 & 0 & {}^0t_{Fy_{k,j}}^{p_{2,k,j}} \\ 0 & 0 & 1 & 0 \\ 0 & 0 & 0 & 1 \end{bmatrix}$$

and

$${}^0\mathbf{H}_{F_{k,j}}^{p_{3,k,j}} = \begin{bmatrix} 1 & 0 & 0 & {}^0t_{Fx_{k,j}}^{p_{3,k,j}} \\ 0 & 1 & 0 & {}^0t_{Fy_{k,j}}^{p_{3,k,j}} \\ 0 & 0 & 1 & 0 \\ 0 & 0 & 0 & 1 \end{bmatrix}.$$

The coefficient matrices for modeling PD induced deviation are shown in the equation at the bottom of the previous page, where $C_1 = q_{2x}^{F_{k,j}} \cdot q_{3y}^{F_{k,j}} - q_{2y}^{F_{k,j}} \cdot q_{3x}^{F_{k,j}} + q_{1y}^{F_{k,j}} \cdot q_{3x}^{F_{k,j}} - q_{1x}^{F_{k,j}} \cdot q_{3y}^{F_{k,j}} - q_{1y}^{F_{k,j}} \cdot q_{2x}^{F_{k,j}} + q_{1x}^{F_{k,j}} \cdot q_{2y}^{F_{k,j}}$, $C_2 = q_{2x}^{F_{k,j}} \cdot q_{3y}^{F_{k,j}} - q_{2y}^{F_{k,j}} \cdot q_{3x}^{F_{k,j}}$, $C_3 = q_{3x}^{F_{k,j}} - q_{2x}^{F_{k,j}}$, $C_4 = q_{3y}^{F_{k,j}} - q_{2y}^{F_{k,j}}$, $C_5 = q_{1x}^{F_{k,j}} \cdot q_{3y}^{F_{k,j}} - q_{1y}^{F_{k,j}} \cdot q_{3x}^{F_{k,j}}$, $C_6 = q_{3x}^{F_{k,j}} - q_{1x}^{F_{k,j}}$, $C_7 = q_{3y}^{F_{k,j}} - q_{1y}^{F_{k,j}}$, $C_8 = q_{1x}^{F_{k,j}} \cdot q_{2y}^{F_{k,j}} - q_{1y}^{F_{k,j}} \cdot q_{2x}^{F_{k,j}}$, $C_9 = q_{2x}^{F_{k,j}} - q_{1x}^{F_{k,j}}$, and $C_{10} = q_{2y}^{F_{k,j}} - q_{1y}^{F_{k,j}}$. Given the nominal HTM for $F_{k,j}$ w.r.t. the LCSs of SD features ($s_{1,k,j}, s_{2,k,j}$) and that of TD feature $t_{k,j}$

$${}^0\mathbf{H}_{F_{k,j}}^{s_{1,k,j}} = \begin{bmatrix} 0 & 0 & 1 & {}^0t_{Fx_{k,j}}^{s_{1,k,j}} \\ 0 & 1 & 0 & {}^0t_{Fy_{k,j}}^{s_{1,k,j}} \\ -1 & 0 & 0 & 0 \\ 0 & 0 & 0 & 1 \end{bmatrix}$$

$${}^0\mathbf{H}_{F_{k,j}}^{s_{2,k,j}} = \begin{bmatrix} 0 & 0 & 1 & {}^0t_{Fx_{k,j}}^{s_{2,k,j}} \\ 0 & 1 & 0 & {}^0t_{Fy_{k,j}}^{s_{2,k,j}} \\ -1 & 0 & 0 & {}^0t_{Fz_{k,j}}^{s_{2,k,j}} \\ 0 & 0 & 0 & 1 \end{bmatrix}$$

and

$${}^0\mathbf{H}_{F_{k,j}}^{t_{k,j}} = \begin{bmatrix} 1 & 0 & 0 & {}^0t_{Fx_{k,j}}^{t_{k,j}} \\ 0 & 0 & 1 & {}^0t_{Fy_{k,j}}^{t_{k,j}} \\ 0 & -1 & 0 & {}^0t_{Fz_{k,j}}^{t_{k,j}} \\ 0 & 0 & 0 & 1 \end{bmatrix}$$

the coefficient matrices for modeling SD and TD induced deviation are shown in the equation at the bottom of this page. For

$$\mathbf{T}_{4,k,j} = \frac{1}{q_{4y}^{F_{k,j}} - q_{5y}^{F_{k,j}}} \begin{bmatrix} 0 & 0 & q_{5y}^{F_{k,j}} & q_{5y}^{F_{k,j}}(q_{4y}^{F_{k,j}} + {}^0t_{Fy_{k,j}}^{s_{1,k,j}}) & -q_{5y}^{F_{k,j}}(q_{4x}^{F_{k,j}} + {}^0t_{Fx_{k,j}}^{s_{1,k,j}}) & 0 \\ 0 & 0 & -q_{6x}^{F_{k,j}} & -q_{6x}^{F_{k,j}}(q_{4y}^{F_{k,j}} + {}^0t_{Fy_{k,j}}^{s_{1,k,j}}) & q_{6x}^{F_{k,j}}(q_{4x}^{F_{k,j}} + {}^0t_{Fx_{k,j}}^{s_{1,k,j}}) & 0 \\ 0 & 0 & 0 & 0 & 0 & 0 \\ 0 & 0 & 0 & 0 & 0 & 0 \\ 0 & 0 & 0 & 0 & 0 & 0 \\ 0 & 0 & 1 & q_{4y}^{F_{k,j}} + {}^0t_{Fy_{k,j}}^{s_{1,k,j}} & -q_{4z}^{F_{k,j}} - {}^0t_{Fx_{k,j}}^{s_{1,k,j}} & 0 \end{bmatrix}$$

$$\mathbf{T}_{5,k,j} = \frac{1}{q_{4y}^{F_{k,j}} - q_{5y}^{F_{k,j}}} \begin{bmatrix} 0 & 0 & -q_{4y}^{F_{k,j}} & q_{4y}^{F_{k,j}}(q_{5y}^{F_{k,j}} + {}^0t_{Fy_{k,j}}^{s_{2,k,j}}) & q_{4y}^{F_{k,j}}(q_{5z}^{F_{k,j}} + {}^0t_{Fx_{k,j}}^{s_{2,k,j}}) & 0 \\ 0 & 0 & q_{6x}^{F_{k,j}} & q_{6x}^{F_{k,j}}(q_{5y}^{F_{k,j}} + {}^0t_{Fy_{k,j}}^{s_{2,k,j}}) & -q_{6x}^{F_{k,j}}(q_{5z}^{F_{k,j}} + {}^0t_{Fx_{k,j}}^{s_{2,k,j}}) & 0 \\ 0 & 0 & 0 & 0 & 0 & 0 \\ 0 & 0 & 0 & 0 & 0 & 0 \\ 0 & 0 & 0 & 0 & 0 & 0 \\ 0 & 0 & -1 & -q_{5y}^{F_{k,j}} - {}^0t_{Fy_{k,j}}^{s_{2,k,j}} & q_{5z}^{F_{k,j}} + {}^0t_{Fx_{k,j}}^{s_{2,k,j}} & 0 \end{bmatrix}$$

$$\mathbf{T}_{6,k,j} = \begin{bmatrix} 0 & 0 & 0 & 0 & 0 & 0 \\ 0 & 0 & -1 & -q_{6y}^{F_{k,j}} - {}^0t_{Fy_{k,j}}^{t_{k,j}} & q_{6x}^{F_{k,j}} + {}^0t_{Fx_{k,j}}^{t_{k,j}} & 0 \\ 0 & 0 & 0 & 0 & 0 & 0 \\ 0 & 0 & 0 & 0 & 0 & 0 \\ 0 & 0 & 0 & 0 & 0 & 0 \\ 0 & 0 & 0 & 0 & 0 & 0 \end{bmatrix}.$$

pin-hole fixturing scheme shown in Fig. 2(b), the nominal HTM for $F_{k,j}$ w.r.t. the LCSs of SD features $(s_{1,k,j}, s_{2,k,j})$ and that of TD feature $t_{k,j}$, are

$$
{}^{0}\mathbf{H}_{F_{k,j}}^{s_{1,k,j}} = \begin{bmatrix} 0 & 0 & 1 & 0 \\ 0 & 1 & 0 & 0 \\ -1 & 0 & 0 & 0 \\ 0 & 0 & 0 & 1 \end{bmatrix}
$$

$$
{}^{0}\mathbf{H}_{F_{k,j}}^{s_{2,k,j}} = \begin{bmatrix} 0 & 0 & 1 & 0 \\ 0 & 1 & 0 & {}^{0}t_{Fy_{k,j}}^{s_{2,k,j}} \\ -1 & 0 & 0 & {}^{0}t_{Fz_{k,j}}^{s_{2,k,j}} \\ 0 & 0 & 0 & 1 \end{bmatrix}
$$

and

$$
{}^{0}\mathbf{H}_{F_{k,j}}^{t_{k,j}} = \begin{bmatrix} 1 & 0 & 0 & 0 \\ 0 & 0 & 1 & 0 \\ 0 & -1 & 0 & 0 \\ 0 & 0 & 0 & 1 \end{bmatrix}
$$

and the coefficient matrices for modeling SD and TD induced deviation will be

$$
\mathbf{T}_{4,k,j}^{*} = \begin{bmatrix} 0 & 0 & -1 & 0 & 0 & 0 \\ 0 & 0 & 0 & 0 & 0 & 0 \\ 0 & 0 & 0 & 0 & 0 & 0 \\ 0 & 0 & 0 & 0 & 0 & 0 \\ 0 & 0 & 0 & 0 & 0 & 0 \\ 0 & 0 & \frac{-1}{q_{5y}^{F_{k,j}}} & 0 & 0 & 0 \end{bmatrix}
$$

$$
\mathbf{T}_{5,k,j}^{*} = \begin{bmatrix} 0 & 0 & 0 & 0 & 0 & 0 \\ 0 & 0 & 0 & 0 & 0 & 0 \\ 0 & 0 & 0 & 0 & 0 & 0 \\ 0 & 0 & 0 & 0 & 0 & 0 \\ 0 & 0 & 0 & 0 & 0 & 0 \\ 0 & 0 & \frac{1}{q_{5y}^{F_{k,j}}} & \frac{\left(q_{5y}^{F_{k,j}} + {}^{0}t_{Fy_{k,j}}^{s_{2,k,j}}\right)}{q_{5y}^{F_{k,j}}} & 0 & 0 \end{bmatrix}
$$

$$
\mathbf{T}_{6,k,j}^{*} = \begin{bmatrix} 0 & 0 & 0 & 0 & 0 & 0 \\ 0 & 0 & -1 & 0 & 0 & 0 \\ 0 & 0 & 0 & 0 & 0 & 0 \\ 0 & 0 & 0 & 0 & 0 & 0 \\ 0 & 0 & 0 & 0 & 0 & 0 \\ 0 & 0 & 0 & 0 & 0 & 0 \end{bmatrix}.
$$

APPENDIX III

This appendix shows the procedure of deriving (27). Substituting the ${}^{N}\mathbf{x}_{k}^{R}$ in (25) for that in (26), we have

$$
\mathbf{x}_k = \mathbf{x}_{k-1} + \mathbf{A}_k^4 \cdot \mathbf{x}_{F_k}^R + {}^{O}\mathbf{u}_k. \tag{A9}
$$

Further substituting the $\mathbf{x}_{F_k}^R$ in (22) for that in (A9), we have

$$
\mathbf{x}_k = \mathbf{x}_{k-1} + \mathbf{A}_k^4 \cdot \left[{}^{D}\mathbf{x}_{F_k}^R + {}^{F}\mathbf{x}_{F_k}^R\right] + {}^{O}\mathbf{u}_k. \tag{A10}
$$

Substituting ${}^{D}\mathbf{x}_{F_k}^R$ in (19) and ${}^{F}\mathbf{x}_{F_k}^R$ in (21) for that in (A10), we have

$$
\begin{aligned}\mathbf{x}_k = \mathbf{x}_{k-1} &+ \mathbf{A}_k^4 \cdot \mathbf{A}_k^2 \cdot \mathbf{A}_k^1 {}^{D}\mathbf{x}_k \\ &+ \mathbf{A}_k^4 \cdot \mathbf{A}_k^2 \cdot {}^{S}\mathbf{u}_k + \mathbf{A}_k^4 \cdot \mathbf{A}_k^3 \cdot {}^{F}\mathbf{u}_k + {}^{O}\mathbf{u}_k.\end{aligned} \tag{A11}
$$

Finally, by substituting ${}^{D}\mathbf{x}_k$ in (17) for that in (A11), we can achieve

$$
\begin{aligned}\mathbf{x}_k = \mathbf{x}_{k-1} &+ \mathbf{A}_k^4 \cdot \mathbf{A}_k^2 \cdot \mathbf{A}_k^1 \cdot \mathbf{A}_k^0 \cdot \mathbf{x}_{k-1} \\ &+ \mathbf{A}_k^4 \cdot \mathbf{A}_k^2 \cdot {}^{S}\mathbf{u}_k + \mathbf{A}_k^4 \cdot \mathbf{A}_k^3 \cdot {}^{F}\mathbf{u}_k + {}^{O}\mathbf{u}_k.\end{aligned} \tag{A12}
$$

This leads to (27).

APPENDIX IV

The acronyms used in the paper are listed here:

MAP	Multistage assembly processes.
KPC	Key product characteristics.
DMV	Differential motion vector.
CS	Coordinate system.
RCS	Reference coordinate system.
FCS	Fixture coordinate system
PCS	Part coordinate system.
LCL	Local coordinate system.
PD	Primary datum.
SD	Secondary datum.
TD	Tertiary datum.

REFERENCES

[1] J. Shi, *Stream of Variation Modeling and Analysis for Multistage Manfuacturing Processes, ISBN: 0-8493-2151-4*. Boca Raton, FL: CRC, Taylor & Francis, 2006, p. 469.

[2] J. F. Lawless, R. J. Mackay, and J. A. Robinson, "Analysis of variation transmission in manufacturing processes—Part I," *J. Qual. Technol.*, vol. 31, no. 2, pp. 131–142, Apr. 1999.

[3] R. Agrawal, J. F. Lawless, and R. J. Mackay, "Analysis of variation transmission in manufacturing processes—Part II," *J. Qual. Technol.*, vol. 31, no. 2, pp. 143–154, Apr. 1999.

[4] R. Mantripragada and D. E. Whitney, "The datum flow chain: A systematic approach to assembly design and modeling," *Res. Eng. Design-Theory Applicat. Concurrent Eng.*, vol. 10, no. 3, pp. 150–165, 1998.

[5] R. Mantripragada and D. E. Whitney, "Modeling and controlling variation propagation in mechanical assemblies using state transition models," *IEEE Trans. Rob. Autom.*, vol. 15, no. 1, pp. 124–140, Feb. 1999.

[6] J. Jin and J. Shi, "State space modeling of sheet metal assembly for dimensional control," *ASME Trans., J. Manuf. Sci. Eng.*, vol. 121, pp. 756–762, 1999.

[7] Q. Huang, J. Shi, and J. Yuan, "Part dimensional error and its propagation modeling in multi-operational machining processes," *ASME Trans. J. Manuf. Sci. Eng.*, vol. 125, pp. 255–262, 2003.

[8] S. Zhou, Q. Huang, and J. Shi, "State space modeling of dimensional variation propagation in multistage machining process using differential motion vectors," *IEEE Trans. Rob. Autom.*, vol. 19, no. 2, pp. 296–309, Apr. 2003.

[9] W. Huang, J. Lin, and Z. Kong, "Stream-of-variation (Sova) modeling II: A generic 3-D variation model for rigid body assembly in multi station assembly processes," *Trans. ASME, J. Manuf. Sci. Eng.*, vol. 129, no. 4, pp. 832–842, 2007.

[10] CETOL 6 Sigma, Sigmetrix LLC, [Online]. Available: http://www.sigmetrix.com/

[11] 3-DCS, Dimensional Control Systems, Inc., [Online]. Available: http://www.3dcs.com

[12] Z. Shen, "Tolerance analysis with EDS/VisVSA," *ASME J. Comput. Inf. Sci. Eng.*, vol. 3, no. 1, pp. 95–99, 2003.

[13] Dimensioning and tolerancing, ANSI/ASME Y14.5M, Amer. Soc. Mech. Eng., 1994.
[14] R. Jayaraman and V. Srinivasan, "Geometric tolerancing: I. Virtual boundary requirements," *IBM J. Res. Develop.*, vol. 33, no. 2, pp. 90–104, 1989.
[15] Y. Wu, J. J. Shah, and J. K. Davidson, "Computer modeling of geometric variations in mechanical parts and assemblies," *ASME J. Comput. Inf. Sci. Eng.*, vol. 3, no. 1, pp. 54–63, 2003.
[16] H. Z. Yau, "Generalization and evaluation of vectorial tolerances," *Int. J. Prod. Res.*, vol. 35, no. 6, pp. 1763–1783, 1997.
[17] R. P. Paul, *Robot Manipulators: Mathematics, Programming, and Control*. Cambridge, MA: MIT Press, 1981, p. 279.
[18] J. Camelio, S. J. Hu, and D. Ceglarek, "Modeling variation propagation of multi-station assembly systems with complaint parts," *ASME Trans. J. Mech. Design*, vol. 125, pp. 673–681, 2003.
[19] M. Chang and D. C. Gossard, "Modeling the assembly of compliant, non-ideal parts," *Comput.-Aided Design*, vol. 29, no. 10, pp. 701–708, 1997.
[20] B. Shiu, D. Ceglarek, and J. Shi, "Flexible beam-based modeling of sheet metal assembly for dimensional control," *Trans. NAMRI/SME*, vol. 25, pp. 49–54, 1997.
[21] S. C. Liu and S. J. Hu, "Variation simulation for deformable sheet metal assemblies using finite element methods," *ASME J. Manuf. Sci. Eng.*, vol. 119, pp. 368–374, 1997.
[22] W. Cai, S. J. Hu, and J. X. Yuan, "A variational method of robust fixture configuration design for 3-D workpieces," *J. Manuf. Sci. Eng.-Trans. ASME*, vol. 119, no. 4A, pp. 593–602, Nov. 1997.
[23] W. Cai, "A new tolerance modeling and analysis methodology through a two-step linearization with applications in automotive body assembly," *J. Manuf. Syst.*, vol. 27, no. 1, pp. 26–35, 2008.
[24] S. Zhou *et al.*, "Diagnosability study of multistage manufacturing processes based on linear mixed-effects models," *Technometrics*, vol. 45, no. 4, pp. 312–325, 2003.

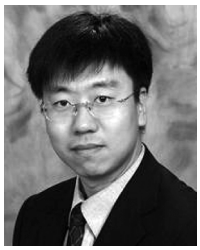

Jian Liu received the B.S. and M.S. degrees in precision instruments and mechanology from the Tsinghua University, Beijing, China, in 1999 and 2002, respectively, and the M.S. degree in industrial engineering, the M.S. degree in statistics, and the Ph.D. degree in mechanical engineering and industrial engineering from the University of Michigan, Ann Arbor, in 2005, 2006, and 2008, respectively.

Currently, he is an Assistant Professor in the Department of Systems and Industrial Engineering at the University of Arizona, Tucson. His research is centered on the integration of manufacturing engineering knowledge, control theory, and advanced statistics for product quality and productivity improvement.

Prof. Liu is a member of INFORMS and IIE.

Jionghua (Judy) Jin (M'06) received the Ph.D. degree in industrial and operations engineering at the University of Michigan, Ann Arbor, in 1999.

Currently, she is an Associate Professor in the Department of Industrial and Operations Engineering at the University of Michigan. Her research focuses on data fusion for quality/reliability improvement, and cost reduction for complex systems. Her expertise is in the areas of complex system modeling for variation analysis and control, automatic feature extraction for monitoring and diagnosis, and integrated design and maintenance policy considering quality and reliability interaction.

Prof. Jin is a member of the ASME, ASQ, IIE, INFORMS, and SME. She has received a number of awards including the Best Paper Awards from ASME, IIE Transactions, and IERC conferences, and a PECASE/CAREER Award from the NSF.

Jianjun Shi received the B.S. and M.S. degrees in electrical engineering from the Beijing Institute of Technology, Beijing, China, in 1984 and 1987, respectively, and the Ph.D. degree in mechanical engineering from the University of Michigan, Ann Arbor, in 1992.

Currently, he is the Carolyn J. Stewart Chair Professor in the H. Milton Stewart School of Industrial and Systems Engineering at the Georgia Institute of Technology, Atlanta. His research interests include the fusion of advanced statistical and domain knowledge to develop methodologies for modeling, monitoring, diagnosis, and control for complex manufacturing systems.

Dr. Shi is a Fellow of the Institute of Industrial Engineers (IIE), a Fellow of American Society of Mechanical Engineers (ASME), a Fellow of The Institute for Operations Research and the Management Sciences (INFORMS) and a member of ASQ, SME, and ASA.